plays a critical role in the development of hypothalamic neurons [5]. *SOX10* mutations are likely to cause gonadotropin deficiency as a sole hormonal defect, because the levels of blood hormones except for E_2 remained grossly normal in our patient.

The results of in vitro assays suggest that *SOX10* mutations lead to the disease phenotype by haploinsufficiency rather than by dominant-negative effects. The broad phenotypic variation of *SOX10* mutation-positive patients can be explained by the notion that haploinsufficiency of developmental genes is usually associated with a wide range of penetrance and expressivity [15].

In conclusion, the present study provides evidence that *SOX10* haploinsufficiency underlies a continuum of developmental defects that includes both HH and WS. Hypothalamic dysfunction appears to be the major hormonal defect resulting from *SOX10* mutations. Further studies will clarify the prevalence and clinical characteristics of *SOX10* abnormalities.

Acknowledgments We thank Dr. Nadege Bondurand and Professor Michel Goossens for providing us the *MITF* reporter vector and the *PAX3* expression vector.

This study was supported by grants from the Ministry of Health, Labor and Welfare, and from Takeda Science Foundation, by Grants-in-Aid for Scientific Research from the Japan Society for the Promotion of Science and from the Ministry of Education, Culture, Sports, Science, and Technology, and by the Grant of National Center for Child Health and Development.

Conflict of interest All the authors declare that there is no conflict of interest.

References

1. R. Rapaport, Disorders of the gonads, in *Nelson textbook of pediatrics*, 18th edn., ed. by R.M. Kliegman, R.E. Behrman, H.B. Jenson, B.F. Stanton (Saunders, Philadelphia, 2007), pp. 2374–2403
2. L.C. Layman, The genetic basis of female reproductive disorders: etiology and clinical testing. Mol. Cell. Endocrinol. **370**(1–2), 138–148 (2013)
3. H. Miraoui, A.A. Dwyer, G.P. Sykiotis, L. Plummer, W. Chung, B. Feng, A. Beenken, J. Clarke, T.H. Pers, P. Dworzynski, K. Keefe, M. Niedziela, T. Raivio, W.F.Jr Crowley, S.B. Seminara, R. Quinton, V.A. Hughes, P. Kumanov, J. Young, M.A. Yialamas, J.E. Hall, G.V. Vliet, J.P. Chanoine, J. Rubenstein, M. Mohammadi, P.S. Tsai, Y. Sidis, K. Lage, N. Pitteloud, Mutations in FGF17, IL17RD, DUSP6, SPRY4, and FLRT3 are identified in individuals with congenital hypogonadotropic hypogonadism. Am. J. Hum. Genet. **92**(5), 725–743 (2013)
4. Y. Izumi, E. Suzuki, S. Kanzaki, S. Yatsuga, S. Kinjo, M. Igarashi, T. Maruyama, S. Sano, R. Horikawa, N. Sato, K. Nakabayashi, K. Hata, A. Umezawa, T. Ogata, Y. Yoshimura, M. Fukami, Genome-wide copy number analysis and systematic mutation screening in 58 patients with hypogonadotropic hypogonadism. Fertil. Steril. (2014). doi:10.1016/j.fertnstert.2014.06.017
5. V. Pingault, V. Bodereau, V. Baral, S. Marcos, Y. Watanabe, A. Chaoui, C. Fouveaut, C. Leroy, O. Vérier-Mine, C. Francannet, D. Dupin-Deguine, F. Archambeaud, F.J. Kurtz, J. Young, J. Bertherat, S. Marlin, M. Goossens, J.P. Hardelin, C. Dodé, N. Bondurand, Loss-of-function mutations in SOX10 cause Kallmann syndrome with deafness. Am. J. Hum. Genet. **92**(5), 707–724 (2013)
6. K. Vaaralahti, J. Tommiska, V. Tillmann, N. Liivak, J. Känsäkoski, E.M. Laitinen, T. Raivio, De novo SOX10 nonsense mutation in a patient with Kallmann syndrome and hearing loss. Pediatr. Res. (2014). doi:10.1038/pr.2014.60
7. V. Pingault, D. Ente, F. Dastot-Le Moal, M. Goossens, S. Marlin, N. Bondurand, Review and update of mutations causing Waardenburg syndrome. Hum. Mutat. **31**(4), 391–406 (2010)
8. M. Iso, M. Fukami, R. Horikawa, N. Azuma, N. Kawashiro, T. Ogata, SOX10 mutation in Waardenburg syndrome type II. Am. J. Med. Genet. A. **146A**(16), 2162–2163 (2008)
9. M. Furukawa, M. Kamide, T. Miwa, R. Umeda, Significance of intravenous olfaction test using thiamine propyldisulfide (Alinamin) in olfactometry. Auris Nasus Larynx **15**(1), 25–31 (1988)
10. T. Tanaka: Endocrine examination. In: T. Tanaka (ed.) New pocket guide of clinical standard values for children. 1st ed., 106-132. Jihou, Tokyo, (2009) [In Japanese]
11. H. Inada, T. Imamura, R. Nakajima: Assessment of pituitary function. In; H. Inada, T. Imamura, R. Nakajima (eds.) Manual of endocrine examinations of children. 2nd ed., 5-22. Medical Review, Osaka, (2002) [In Japanese]
12. N. Bondurand, V. Pingault, D.E. Goerich, N. Lemort, E. Sock, C.L. Caignec, M. Wegner, M. Goossens, Interaction among SOX10, PAX3 and MITF, three genes altered in Waardenburg syndrome. Hum. Mol. Genet. **9**(13), 1907–1917 (2000)
13. H. Zhang, H. Chen, H. Luo, J. An, L. Sun, L. Mei, C. He, L. Jiang, W. Jiang, K. Xia, J.D. Li, Y. Feng, Functional analysis of Waardenburg syndrome-associated PAX3 and SOX10 mutations: report of a dominant-negative SOX10 mutation in Waardenburg syndrome type II. Hum. Genet. **131**(3), 491–503 (2012)
14. B. Jelena, L. Christina, V. Eric, Q.R. Fabiola, Phenotypic variability in Waardenburg syndrome resulting from a 22q12.3-q13.1 microdeletion involving SOX10. Am. J. Med. Genet A. **164**(6), 1512–1519 (2014)
15. E. Fisher, P. Scambler, Human haploinsufficiency-one for sorrow, two for joy. Nat. Genet. **7**(1), 5–7 (1994)

ORIGINAL RESEARCH ARTICLE | Genetics inMedicine

Open

The natural history of MPS I: global perspectives from the MPS I Registry

Michael Beck, MD[1], Pamela Arn, MD[2], Roberto Giugliani, MD, PhD, MSc[3], Joseph Muenzer, MD, PhD[4], Torayuki Okuyama, MD, PhD[5], John Taylor, MS[6] and Shari Fallet, DO[6]

Purpose: In this study, we aimed to describe the natural history of mucopolysaccharidosis I.

Methods: Data from 1,046 patients who enrolled in the MPS I Registry as of August 2013 were available for descriptive analysis. Only data from untreated patients and data prior to treatment for patients who received treatment were considered. Age at symptom onset, diagnosis, and treatment initiation were examined by geographic region and phenotype (from most to least severe: Hurler, Hurler–Scheie, and Scheie). For each symptom, frequency and age at onset were examined.

Results: Natural history data were available for 987 patients. Most patients were from Europe (45.5%), followed by North America (34.8%), Latin America (17.3%), and Asia Pacific (2.4%). Phenotype distribution was 60.9% for Hurler, 23.0% for Hurler–Scheie, and 12.9% for Scheie (3.2% undetermined) syndromes. Median age at symptom onset for Hurler, Hurler–Scheie, and Scheie syndromes was 6 months, 1.5 years, and 5.3 years, respectively; median age at treatment initiation was 1.5 years, 8.0 years, and 16.9 years, respectively. Coarse facial features and corneal clouding were among the most common symptoms in all three phenotypes.

Conclusion: A delay between symptom onset and treatment exists, especially in patients with attenuated mucopolysaccharidosis I. A better understanding of disease manifestations may help facilitate prompt diagnosis and treatment and improve patient outcomes.

Genet Med advance online publication 27 March 2014

Key Words: MPS I; natural history; registry; symptoms

INTRODUCTION

Mucopolysaccharidosis type I (MPS I) is a rare autosomal recessive disease caused by a deficiency of α-L-iduronidase, an enzyme required for the degradation of the glycosaminoglycans dermatan and heparan sulfate. The estimated incidence of MPS I is 1 in every 100,000 live births. Due to the chronic and progressive accumulation of glycosaminoglycans in the lysosomes of cells throughout the body, patients affected by this devastating disease experience multiorgan dysfunction leading to considerable morbidity in most patients, and early mortality in those most severely affected.[1]

Like most other metabolic inherited diseases, MPS I displays significant variability in its presentation and course. This may be due to differences among patients in the severity of the underlying mutation(s) and consequent degree of residual enzyme activity; however, other factors may also contribute to the well-known phenotypic heterogeneity.[2] Historically, MPS I has been classified into three syndromes—Hurler, Hurler–Scheie, and Scheie—though it is now widely accepted that overlap in symptomatology exists among these subtypes.[1] Hurler syndrome, the most severe form of MPS I, typically involves significant developmental delay and cognitive decline, along with characteristic coarse facial features, joint stiffness and contractures, short stature, and respiratory, cardiac, and hepatic disease. Symptoms emerge shortly after birth and progress rapidly, such that most patients with Hurler syndrome die within the first decade of life. At the other end of the MPS I disease spectrum, Scheie syndrome involves later onset of typically milder symptoms and a slower disease progression. While patients with the Scheie phenotype usually develop significant disease-related morbidity, they show normal intelligence and survive into adulthood. Hurler–Scheie syndrome represents an intermediate phenotype that is characterized by mild or no cognitive impairment but includes somatic symptoms that reduce life expectancy into the second or third decade of life. Delineation of the different MPS I phenotypes can be challenging and is largely driven by consideration of the age of symptom onset and rate of disease progression as well as a patient's genotype.[3]

Historically, treatment of MPS I was restricted to palliative care and symptom-based interventions, including surgery (e.g., adenotonsillectomy, hernia repair, ventriculoperitoneal shunt, cardiac valve replacement, carpal tunnel release, and spinal decompression); physical, occupational, and speech therapies; respiratory support; hearing aids; and medications for pain and gastrointestinal disturbances. Since 1981, hematopoietic stem cell transplantation (HSCT) has been used to treat MPS I. When successful, it is a one-time procedure that can prolong survival, preserve cognitive function, and reduce some somatic features of the disease.[4,5] However, due to its significant

[1]Children's Hospital, University of Mainz, Mainz, Germany; [2]The Nemours Children's Clinic, Jacksonville, Florida, USA; [3]Department of Genetics UFRGS and INAGEMP, Medical Genetics Service/HCPA, Porto Alegre, Rio Grande do Sul, Brazil; [4]University of North Carolina at Chapel Hill, Chapel Hill, North Carolina, USA; [5]National Center for Child Health and Development, Tokyo, Japan; [6]Genzyme, a Sanofi company, Cambridge, Massachusetts, USA. Correspondence: Michael Beck (Michael.Beck@unimedizin-mainz.de)

Submitted 17 December 2013; accepted 7 February 2014; advance online publication 27 March 2014. doi:10.1038/gim.2014.25

morbidity, HSCT is reserved for patients with the most severe form of MPS I, Hurler syndrome. HSCT is typically recommended for patients under 2 years of age with normal cognition (intelligence quotient >70) because early intervention increases the likelihood of maintaining cognitive abilities. For patients with Hurler–Scheie and Scheie syndromes, enzyme replacement therapy (ERT) with laronidase (recombinant human α-L-iduronidase; Aldurazyme) is the primary treatment option.[6–10] Laronidase is administered weekly via intravenous infusion and is a lifelong therapy.

The success of both HSCT and ERT may depend on early initiation of treatment. Developmental outcomes are better when transplantation is performed before 24 months of age,[11] and laronidase may also be more beneficial when started early in life, based on the suggestion from two case reports on siblings with Hurler–Scheie syndrome.[12,13] Unfortunately, early diagnosis (and hence early initiation of treatment) is limited by several factors, including the rarity of the disease, the wide variability in clinical presentation and disease course, and the nonspecific nature of some of the early manifestations of the disease. As is true of other rare genetic diseases, MPS I awareness among physicians is also hampered by a general lack of familiarity with its symptoms and course.

With the advent of several potentially lifesaving therapies, the need for better disease recognition and early diagnosis is heightened. The MPS I Registry (ClinicalTrials.gov identifier: NCT00144794) is a global, observational disease database established in 2003 by Genzyme/BioMarin and is maintained by Genzyme, a Sanofi company.[12] The collection of data in the Registry is aimed at facilitating characterization of the course of disease and tracking clinical outcomes in patients with MPS I. In addition, participating health-care professionals are provided access to aggregate data on MPS I and can query the database for specific information to facilitate the care of their patients with MPS I. Analyses of data from the Registry have provided insights about disease burden, genotype–phenotype correlations, frequency and risks of surgical procedures, and changing treatment trends in MPS I patients.[13–15] The intent of this analysis is to use data from the Registry to describe the natural history of MPS I by phenotype and across regions in an effort to improve the recognition and prompt diagnosis of this potentially fatal, but treatable, disease.

MATERIALS AND METHODS

The global MPS I Registry was initiated in April 2003 as part of an effort to help health-care professionals involved in the diagnosis and treatment of MPS I better understand the disease and its management and to help create MPS I disease treatment monitoring guidelines. All data provided for this analysis were obtained as of August 2013. Patient participation in the MPS I Registry is voluntary. Each independent site is responsible for obtaining a patient's informed consent for submitting his/her health information to the Registry and for using and disclosing this information in subsequent aggregate analyses, such as journal articles, annual reports, educational materials, and public health reports. Historically, each independent site has been responsible for determining whether site-specific institutional review board or ethics committee review is required for participation in the Registry in accordance with institutional policies and local laws and regulations. Since December 2012, the MPS I Registry protocol has required sites to submit to and receive approval from an institutional review board or ethics committee. All patient data are anonymized and entered by participating sites in accordance with applicable privacy regulations. At enrollment, detailed medical histories and baseline data are collected and physicians are encouraged to follow a recommended schedule of clinical assessments and regularly report the results of their assessments.[12]

This report is based on Registry data as of August 2013, at which time information was available for 1,046 patients. The Registry includes comprehensive information for treated as well as untreated patients; for the treated patients, data are available from the periods prior to, during, and/or subsequent to treatment. Therefore, a definition of the natural history period and the following patient inclusion criteria were used to select data for the analyses presented here: (i) Known ERT status, (ii) For patients receiving ERT, known date of first infusion, (iii) Known HSCT status, and (iv) For patients who had received HSCT, known date of transplant.

From the initial cohort of 1,046 patients, 987 patients met the inclusion criteria. For patients who had never been treated, the natural history period was defined as the time from birth to the last follow-up recorded in the Registry. Among patients who had been treated with ERT, HSCT, or both, the natural history period was defined as the time from birth to first treatment (either ERT or HSCT).

Ages at first symptom, diagnosis, and treatment initiation (where applicable) were evaluated by region and MPS I phenotype. Symptom prevalence and age of onset of symptoms relating to general appearance and neurologic, cardiac, respiratory, gastrointestinal, and musculoskeletal status were evaluated by phenotype. Only the symptoms observed during the predefined natural history period were considered. Given that not all patients had data reported for every symptom during the natural history period, the assumption was made that symptoms not explicitly reported were not present, and frequencies were calculated as the number of patients with the symptom present divided by all patients in each region and/or phenotype. This assumption means that the reported frequencies may underestimate the true frequency for each symptom. Descriptive statistics were computed for age of onset of each symptom (as indicated by the earliest age each symptom was reported) among patients who experienced the symptom. For those patients with the same symptom reported multiple times, the earliest age was used, corresponding to "onset" or "age first reported."

RESULTS

Global occurrence of MPS I phenotypes

A total of 987 MPS I patients with evaluable natural history information were enrolled in the Registry as of August 2013

(Table 1). The largest proportion of patients was from Europe (45.5%), with the next largest from North America (34.8%), followed by Latin America (17.3%) and Asia Pacific (2.4%).

The overall phenotypic distribution was 601 (60.9%) for Hurler, 227 (23.0%) for Hurler–Scheie, and 127 (12.9%) for Scheie. Another 32 (3.2%) patients met the criteria for inclusion in this analysis, but their phenotypes were not reported in the Registry and were therefore considered undetermined or missing. Of note, North America (71.4%) and Europe (61.5%) had higher proportions of patients with the severe Hurler phenotype than Latin America (42.7%) or the Asia Pacific region (29.2%).

Chronology of symptom onset, diagnosis, and treatment by region

Median ages at symptom onset, MPS I diagnosis, and first treatment (ERT or HSCT, if applicable) are presented by region and phenotype in Figure 1. Across all regions, patients with Hurler syndrome, the most severe phenotype, were diagnosed and treated earliest, as expected. The median age at symptom onset for these patients was 6 months, and diagnosis and treatment initiation followed quickly thereafter, at median ages of 12 and 18 months, respectively. Patients with Hurler–Scheie and Scheie syndromes, which have the more attenuated presentations, typically experienced initial symptoms sometime after infancy and exhibited a 2- to 4-year gap between onset of symptoms and diagnosis, respectively, and a 4- to 8-year gap between diagnosis and treatment initiation, respectively.

Analyses of age of symptom onset, diagnosis, and treatment initiation based on phenotype and geographic region generally mirrored the results in the overall Registry population, with a few notable exceptions. In North America, treatment initiation for patients with Scheie syndrome was earlier than in the other regions. The median age for treatment initiation for patients diagnosed with Scheie syndrome in North America was 11.7 years, whereas in Europe and Latin America it was 16.9 and 17.7 years, respectively. The Asia Pacific region had an even higher median age of 31.5 years for treatment initiation. The median age of treatment initiation in patients with Hurler–Scheie was also higher in the Asia Pacific region (23.8 years) compared with the overall Registry population (8 years). Another notable finding was the rate of patients with an undetermined or missing phenotype in Latin America (11.1%), which was much higher compared with the other regions. The median ages of symptom onset, diagnosis, and treatment initiation for patients in Latin America with an undetermined phenotype were 0.7, 1.3, and 3.3 years, respectively, which is highly comparable to the median ages for patients in Latin America with the Hurler phenotype (0.7, 1.7, and 3.6 years, respectively), suggesting that some portion of the patients with undetermined phenotypes may, in fact, have Hurler syndrome.

Natural history of MPS I by phenotype

Symptom frequency by phenotype. Coarse facial features were the most predominant characteristic of all functional and anatomic abnormalities for both the Hurler and the Hurler–Scheie phenotypes, occurring in 86.4 and 72.7% of these patients, respectively. The symptoms occurring in at least 25% of patients are summarized by phenotype in Figure 2, and all symptoms, including those occurring in less than 25% of patients, are summarized by phenotype in **Supplementary Table S1** online. Among patients with the Scheie phenotype, 48.0% presented with coarse facial features. Corneal clouding was noted in all three phenotypes at approximately the same rate: 70.9, 68.3, and 70.1% for Hurler, Hurler–Scheie, and Scheie, respectively.

Hepatomegaly was present in the majority of patients with Hurler (70.0%) and Hurler–Scheie (66.5%) phenotypes and in approximately half (48.0%) of those with the Scheie phenotype. Similarly, splenomegaly was present in 50.9% of patients with Hurler syndrome and 47.1% of patients with Hurler–Scheie syndrome but in only 27.6% of those with the Scheie phenotype. The incidences of hernias were more evenly distributed among the phenotypic groups, with 58.9% in Hurler, 59.9% in Hurler–Scheie, and 53.5% in Scheie patients.

In terms of musculoskeletal abnormalities, kyphosis/gibbus was the only abnormality present in the majority (70.0%) of patients with Hurler phenotype, and it was reported much less frequently in patients with Hurler–Scheie (33.5%) and Scheie (21.3%) phenotypes. Conversely, joint contractures and carpal tunnel syndrome were present in the majority of Scheie patients (69.3 and 51.2%, respectively) but were less common in Hurler–Scheie patients (57.3 and 27.8%, respectively) and even less frequent in Hurler patients (37.9 and 7.8%, respectively).

Cardiac valve abnormalities were observed in 67.7% of Scheie patients, 59.0% of Hurler–Scheie patients, and 48.9% of

Table 1 Distribution of MPS I phenotypes by geographic region—all evaluable patients

Geographic region	Hurler,[a] *n* (%)	Hurler–Scheie,[a] *n* (%)	Scheie,[a] *n* (%)	Undetermined,[a] *n* (%)	Total,[b] *n* (%)
All regions	601 (60.9)	227 (23.0)	127 (12.9)	32 (3.2)	987
Asia Pacific	7 (29.2)	5 (20.8)	12 (50.0)	0	24 (2.4)
Europe	276 (61.5)	102 (22.7)	63 (14.0)	8 (1.8)	449 (45.5)
Latin America	73 (42.7)	57 (33.3)	22 (12.9)	19 (11.1)	171 (17.3)
North America	245 (71.4)	63 (18.4)	30 (8.7)	5 (1.5)	343 (34.8)

MPS I, mucopolysaccharidosis type I.

[a]Percentages are based on the number of patients in each region enrolled in the Registry who met the criteria for inclusion in this analysis as of 2 August 2013.

[b]Percentages are based on the number of patients in all regions enrolled in the Registry who met the criteria for inclusion in this analysis as of 2 August 2013.

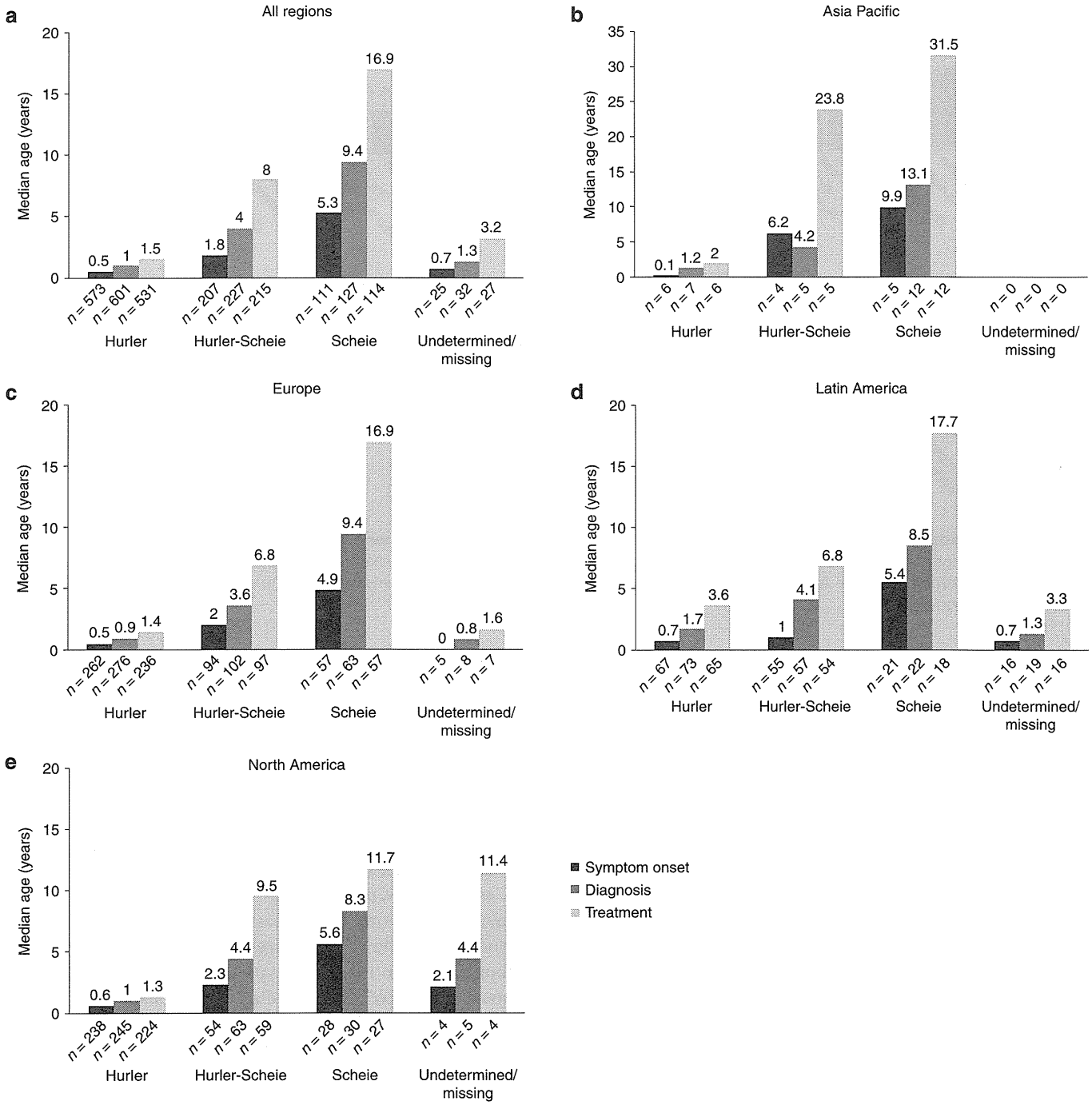

Figure 1 Median age of onset of symptoms, diagnosis, and treatment by phenotype. (**a**) All regions, (**b**) Asia Pacific, (**c**) Europe, (**d**) Latin America, and (**e**) North America. Median age in years (left axis) calculated on the basis of patients within each phenotype for whom age of symptom onset, diagnosis, or treatment was recorded. The median age in years is noted above each column. The number of patients, *n*, is noted below each column. In **b**, the median age of symptom onset is higher than the median age of diagnosis for the five Hurler–Scheie patients, even though all five had an age of symptom onset less than or equal to the age at diagnosis, because data for age of symptom onset were not available for one patient.

Hurler patients. Airway-related symptoms, such as sleep disturbances/snoring were observed in 51.6% of Hurler patients, 48.9% of Hurler–Scheie patients, and 26.8% of Scheie patients. Cognitive impairment was observed in 46.4, 31.3, and 9.4% of patients with Hurler, Hurler–Scheie, and Scheie phenotypes, respectively.

Age of symptom onset by phenotype

As expected, first symptoms appeared earlier (within the first 2 years of life) in patients with the Hurler phenotype; whereas, in patients with the Hurler–Scheie and Scheie phenotypes, commonly occurring symptoms were first observed between 3 and 7, and 5 and 13 years of age, respectively. The median ages of

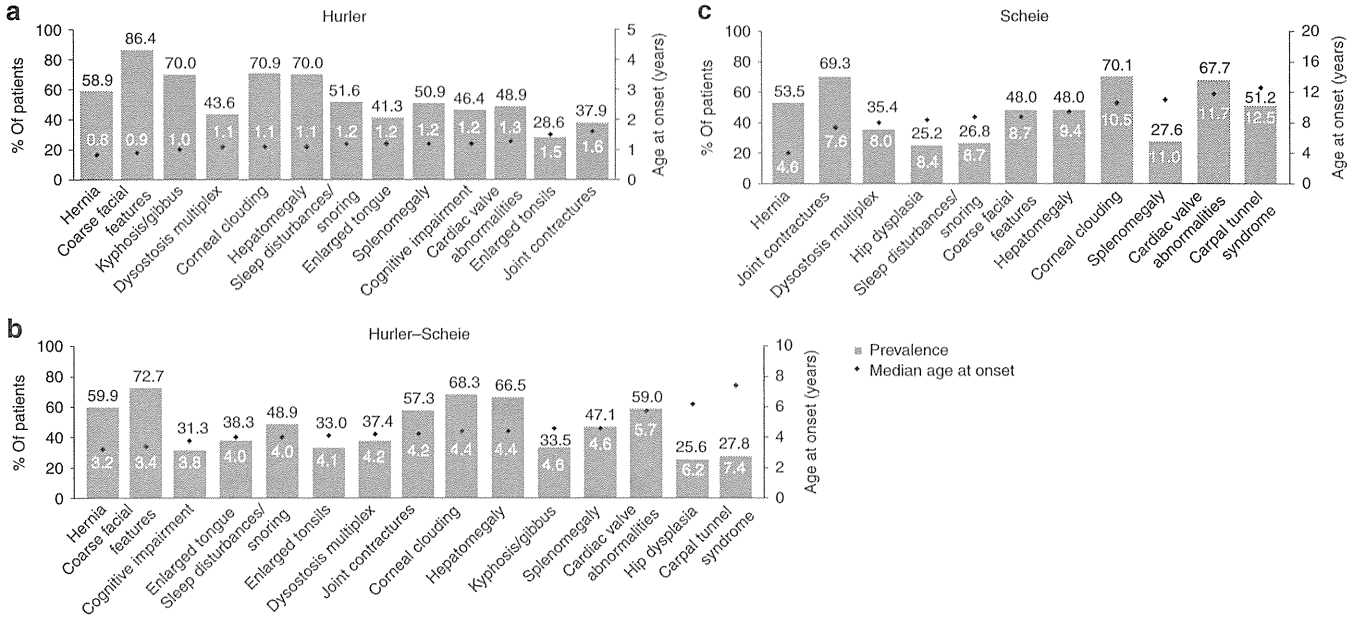

Figure 2 Prevalence and age of onset of signs and symptoms in patients with MPS I by phenotype. (**a**) Hurler, (**b**) Hurler–Scheie, and (**c**) Scheie. Percentages of symptom frequency are shown on the left axis. Only symptoms reported during the natural history period in at least 25% of patients with the relevant phenotype are shown. Age data are median ages in years (right axis) for those patients with the date of symptom onset recorded. MPS I, mucopolysaccharidosis type I.

onset of symptoms occurring in at least 25% of patients are presented by phenotype in Figure 2, and the median ages of onset of all symptoms, including those occurring in less than 25% of patients, are summarized by phenotype in **Supplementary Table S2** online.

Across all phenotypes, hernias were the earliest reported symptom, which was noted at median ages of 0.8, 3.2, and 4.6 years of age in Hurler, Hurler–Scheie, and Scheie patients, respectively. Coarse facial features, the most prevalent symptom in patients with Hurler and Hurler–Scheie phenotypes, were also an early finding, with a median age at onset of 0.9 years in Hurler patients and 3.4 and 8.7 years in patients with Hurler–Scheie and Scheie phenotypes, respectively. Corneal clouding, the most prevalent symptom in patients with the Scheie phenotype, was first noted at a median age of 10.5 years in that subset of patients.

Among patients with the Hurler phenotype, kyphosis/gibbus had a median age at onset of 1.0 year (Figure 2a), and dysostosis multiplex, corneal clouding, and hepatomegaly had a median age at onset of 1.1 years. Several symptoms, including sleep disturbances/snoring, enlarged tongue, cognitive impairment, and splenomegaly had a median age at onset of 1.2 years, whereas cardiac valve abnormalities were noted at a median age of 1.3 years. The symptoms that appeared latest in at least 25% of patients with Hurler syndrome were enlarged tonsils and joint contractures, with a median age at onset of 1.5 and 1.6 years, respectively.

The symptoms reported in Hurler–Scheie patients are shown in Figure 2b. After hernias and coarse facial features, cognitive impairment was the earliest symptom observed, first occurring at a median age of 3.8 years. The median ages of onset for enlarged tongue, sleep disturbances/snoring, enlarged tonsils, joint contractures, and dysostosis multiplex were between 4.0 and 4.2 years. Both corneal clouding and hepatomegaly had a median age at onset of 4.4 years, whereas splenomegaly and kyphosis/gibbus had a median age at onset of 4.6 years. Symptoms appearing later in patients with the Hurler–Scheie phenotype included cardiac valve abnormalities, hip dysplasia, and carpal tunnel syndrome, with median ages at onset of 5.7, 6.2, and 7.4 years, respectively.

Symptoms reported in at least 25% of patients with Scheie phenotype are shown in Figure 2c. After hernias, the earliest symptoms within this phenotype were joint contractures and dysostosis multiplex, with median ages at onset of 7.6 and 8.0 years, respectively. Hip dysplasia was first reported at a median age of 8.4 years. Both sleep disturbances/snoring and coarse facial features had a median age at onset of 8.7 years, and hepatomegaly was observed at a median age of 9.4 years. Symptoms appearing later included corneal clouding at 10.5 years, splenomegaly at 11.0 years, cardiac valve abnormalities at 11.7 years, and carpal tunnel syndrome at 12.5 years.

DISCUSSION

MPS I is a rare panethnic genetic disorder characterized by a spectrum of disease with variable age of onset, progression, and organ involvement. If left untreated, patients with the most severe phenotype experience progressive deterioration of the musculoskeletal, cardiorespiratory, and central nervous systems and, typically, die before the age of 10 years.[1] Although patients with the least severe phenotype usually have normal

cognitive functioning and survive into adulthood, more than 50% may be affected by cardiac valve abnormalities, joint contractures, corneal clouding, hernias, and hepatomegaly.[15] The availability of improved disease-specific treatments, including HSCT and ERT, allows patients affected with MPS I to obtain substantial clinical benefit for many disease manifestations, including hepatosplenomegaly, upper airway obstruction (including sleep apnea), cardiac symptoms, and coarse facial features.[3] Importantly, the chances of success from these treatments is improved when initiated prior to the onset of irreversible organ damage.

Due to the rarity of the disease as well as the variability of clinical manifestations, MPS I poses challenges for diagnosis. The MPS I Registry provides the largest global data set for evaluating the natural history, clinical presentation, and potential treatment response of patients with MPS I.

The phenotypic distribution in the Registry data set, with most patients (60.9%) in the most severe phenotypic category, Hurler, and the remaining more attenuated phenotypes, Hurler–Scheie (23%) and Scheie (12.9%), is consistent with existing data, suggesting that ~50–80% of patients have severe MPS I.[4] However, the observed rates of the various phenotypes within the Registry may have been impacted by selection bias; e.g., more attenuated phenotypes could be underrepresented due to preferential identification and enrollment of patients with more severe clinical presentations. In an effort to minimize selection bias, the Registry accepts all patients with a diagnosis of MPS I, regardless of treatment status.[12]

Regional differences in phenotypic distribution were also noted. North America and Europe had higher proportions of patients with the Hurler phenotype than did Latin America or the Asia Pacific region. These regional differences could be due to differences in the "genetic landscape" in different geographic regions or may be the result of regional differences in identification and enrollment of MPS I patients in this voluntary Registry. Some evidence exists for regional genetic differences, in that certain severe mutations (common nonsense mutations) identified in North America and Europe have not been observed in the Asia Pacific region.[2] The profile of MPS I mutations in Brazil also differs from that found in other regions.[16] Based on the similarities in median ages of symptom onset, diagnosis, and treatment initiation, the present study suggests that a substantial proportion of patients in Latin America whose phenotypes were classified as undetermined/missing could have Hurler syndrome.

Early symptom recognition and diagnosis are essential to achieve the best long-term prognosis in patients with MPS I. It is of paramount importance that not only pediatricians, but other specialists as well, are familiar with the clinical manifestations and consider an MPS diagnosis, especially when symptoms are present in combination with each other. Hernias were the earliest presenting symptoms in all three phenotypes. Therefore, the presence of inguinal or umbilical hernias in young children should raise suspicion of MPS I. Likewise, coarse facial features, which are early manifestations and the most prevalent symptom in patients with Hurler and Hurler–Scheie phenotypes, should be considered as an early sign of a potential MPS I diagnosis. Corneal clouding is also a highly prevalent and relatively early manifestation of MPS I across the phenotypes.

Our findings indicate significant delays in diagnosis and treatment, particularly in patients with attenuated phenotypes. Regional differences were evident as well, with attenuated patients in Asia Pacific receiving treatment 18–22 years following the onset of symptoms—a 10- to 12-year delay compared with the 6–12 years between onset of symptoms and treatment in the overall Registry population. This delay may be due, in part, to a lack of access to ERT in some countries.

The data presented here confirm findings from a previous analysis of Registry data published in 2007, shortly after the Registry was established.[12] The current analyses are based on a much larger set of patients (987 vs. 302), provide global and regional breakdowns of the data, and include data from the natural history period only. Regardless, and not surprisingly, there are similarities between the two reports in the age at symptom onset, age at diagnosis, and the rates of prevalence of common MPS I symptoms. However, the current report, based on data from a larger number of patients, provides a more detailed and refined analysis of the earlier findings.

When interpreting results of data analyses from the MPS I Registry, certain limitations common to observational registries should be considered.[17,18] As with any voluntary registry, incomplete or missing data may affect the results, though a recent analysis of the MPS I Registry using source document verification revealed an overall source-to-database error rate of <4%, with no systematic errors.[19] It is also possible that assessment and data collection methods at the participating sites around the world may not be sufficiently standardized and/or that Registry enrollment biases, perhaps based on regional disease classification, symptom severity, and symptom reporting practices, affected the results. For example, patients who did not have a particular symptom may not have had any information reported for that symptom (i.e., rather than indicating that a patient did not have a symptom, the investigator did not provide information about that symptom). This possibility led us to calculate symptom prevalence rates as the number of patients with a particular reported symptom divided by the total number of patients in each region and/or phenotype. As a consequence, the true symptom prevalence rates are at least what we have calculated, and may be higher. In this study, a slightly higher than expected number of patients with attenuated MPS I had cognitive impairment (31.3% of Hurler–Scheie and 9.4% of Scheie patients). This likely reflects the fact that MPS I presents as a disease continuum, making phenotypic classification of MPS I somewhat subjective. Thus, it is possible that some Hurler and Hurler–Scheie patients may have been misclassified as Hurler–Scheie and Scheie phenotypes, respectively. Although the aforementioned potential limitations are not insignificant, the data compiled in the MPS I

Registry are clearly valuable for drawing inferences and generating hypotheses.

Conclusions

The MPS I Registry is the largest global database of information from MPS I patients and provides a useful tool for expanding knowledge about disease presentation, clinical status, and treatment outcomes. Greater understanding of the symptomatology of the disease can lead to earlier diagnosis and initiation of treatment, which may in turn lead to better patient outcomes. Each of the three MPS I phenotypes, Hurler, Hurler–Scheie, and Scheie, is associated with a characteristic constellation of symptoms and disease course. This analysis of data from almost 1,000 patients facilitates definition of the natural history of MPS I across the phenotypic spectrum, which will hopefully increase awareness of the disease and improve early diagnosis. In addition, results from this investigation will be important in establishing benchmarks for future analyses of treatment interventions.

SUPPLEMENTARY MATERIAL

Supplementary material is linked to the online version of the paper at http://www.nature.com/gim

ACKNOWLEDGMENTS

The authors are grateful to Kathleen Melia, PhD, SRSC, LLC, for assistance with medical writing, and to Lisa Underhill, MS, and Iva Ivanovska Holder, PhD, Genzyme Global Medical Affairs, for critical review of the manuscript. This study was funded by Genzyme, a Sanofi company.

DISCLOSURE

M.B. received unrestricted grants, honoraria, and travel support from Genzyme, Shire, Biomarin Pharmaceutical, and Actelion. P.A. is the Chair of the North American Board of Advisors and a member of the International Board of Advisors for the MPS I Registry. R.G. received travel grants and/or speaker honoraria from Genzyme to participate in scientific meetings and investigator fees for his participation in Genzyme-sponsored clinical trials. J.M. received honoraria, educational, and travel grants from Janssen R&D, Shire, and GreenCross and has participated in clinical trials with BioMarin Phamaceutical, Genzyme, and Shire. T.O. received speaker honoraria from Genzyme to participate in scientific meetings. J.T. and S.F. are employees of Genzyme, a Sanofi company.

REFERENCES

1. Neufeld EF, Muenzer J. The mucopolysaccharidoses. In: Scriver C, Beaudet A, Sly W, et al. (eds) *The Metabolic and Molecular Bases of Inherited Disease.* McGraw Hill: New York, NY, 2001:3421–3452.
2. Terlato NJ, Cox GF. Can mucopolysaccharidosis type I disease severity be predicted based on a patient's genotype? A comprehensive review of the literature. *Genet Med* 2003;5:286–294.
3. Muenzer J, Wraith JE, Clarke LA; International Consensus Panel on Management and Treatment of Mucopolysaccharidosis I. Mucopolysaccharidosis I: management and treatment guidelines. *Pediatrics* 2009;123:19–29.
4. Peters C, Balthazor M, Shapiro EG, et al. Outcome of unrelated donor bone marrow transplantation in 40 children with Hurler syndrome. *Blood* 1996;87:4894–4902.
5. Peters C, Shapiro EG, Anderson J, et al. Hurler syndrome: II. Outcome of HLA-genotypically identical sibling and HLA-haploidentical related donor bone marrow transplantation in fifty-four children. The Storage Disease Collaborative Study Group. *Blood* 1998;91:2601–2608.
6. Kakkis ED, Muenzer J, Tiller GE, et al. Enzyme-replacement therapy in mucopolysaccharidosis I. *N Engl J Med* 2001;344:182–188.
7. Wraith JE, Clarke LA, Beck M, et al. Enzyme replacement therapy for mucopolysaccharidosis I: a randomized, double-blinded, placebo-controlled, multinational study of recombinant human alpha-L-iduronidase (laronidase). *J Pediatr* 2004;144:581–588.
8. Sifuentes M, Doroshow R, Hoft R, et al. A follow-up study of MPS I patients treated with laronidase enzyme replacement therapy for 6 years. *Mol Genet Metab* 2007;90:171–180.
9. Wraith JE, Beck M, Lane R, et al. Enzyme replacement therapy in patients who have mucopolysaccharidosis I and are younger than 5 years: results of a multinational study of recombinant human alpha-L-iduronidase (laronidase). *Pediatrics* 2007;120:e37–e46.
10. Clarke LA, Wraith JE, Beck M, et al. Long-term efficacy and safety of laronidase in the treatment of mucopolysaccharidosis I. *Pediatrics* 2009;123:229–240.
11. Peters C, Balthazor M, Shapiro EG, et al. Outcome of unrelated donor bone marrow transplantation in 40 children with Hurler syndrome. *Blood* 1996;87:4894–4902.
12. Pastores GM, Arn P, Beck M, et al. The MPS I registry: design, methodology, and early findings of a global disease registry for monitoring patients with Mucopolysaccharidosis Type I. *Mol Genet Metab* 2007;91:37–47.
13. D'Aco K, Underhill L, Rangachari L, et al. Diagnosis and treatment trends in mucopolysaccharidosis I: findings from the MPS I Registry. *Eur J Pediatr* 2012;171:911–919.
14. Arn P, Wraith JE, Underhill L. Characterization of surgical procedures in patients with mucopolysaccharidosis type I: findings from the MPS I Registry. *J Pediatr* 2009;154:859–64.e3.
15. Thomas JA, Beck M, Clarke JT, Cox GF. Childhood onset of Scheie syndrome, the attenuated form of mucopolysaccharidosis I. *J Inherit Metab Dis* 2010;33:421–427.
16. Matte U, Leistner S, Lima L, Schwartz I, Giugliani R. Unique frequency of known mutations in Brazilian MPS I patients. *Am J Med Genet* 2000;90:108–109.
17. Temple R. Problems in the use of large data sets to assess effectiveness. *Int J Technol Assess Health Care* 1990;6:211–219.
18. Canto JG, Kiefe CI, Williams OD, Barron HV, Rogers WJ. Comparison of outcomes research with clinical trials using preexisting data. *Am J Cardiol* 1999;84:923–7, A6.
19. Verhulst K, Artiles-Carloni L, Beck M, et al. Source document verification in the Mucopolysaccharidosis Type I Registry. *Pharmacoepidemiol Drug Saf* 2012;21:749–752.

Hum Genet (2014) 133:225–234
DOI 10.1007/s00439-013-1372-6

ORIGINAL INVESTIGATION

A hemizygous *GYG2* mutation and Leigh syndrome: a possible link?

Eri Imagawa · Hitoshi Osaka · Akio Yamashita · Masaaki Shiina · Eihiko Takahashi · Hideo Sugie · Mitsuko Nakashima · Yoshinori Tsurusaki · Hirotomo Saitsu · Kazuhiro Ogata · Naomichi Matsumoto · Noriko Miyake

Received: 17 April 2013 / Accepted: 29 September 2013 / Published online: 8 October 2013

Abstract Leigh syndrome (LS) is an early-onset progressive neurodegenerative disorder characterized by unique, bilateral neuropathological findings in brainstem, basal ganglia, cerebellum and spinal cord. LS is genetically heterogeneous, with the majority of the causative genes affecting mitochondrial malfunction, and many cases still remain unsolved. Here, we report male sibs affected with LS showing ketonemia, but no marked elevation of lactate and pyruvate. To identify their genetic cause, we performed whole exome sequencing. Candidate variants were narrowed down based on autosomal recessive and X-linked recessive models. Only one hemizygous missense mutation (c.665G>C, p.W222S) in glycogenin-2 (*GYG2*) (isoform a: NM_001079855) in both affected sibs and a heterozygous change in their mother were identified, being consistent with the X-linked recessive trait. *GYG2* encodes glycogenin-2 (GYG2) protein, which plays an important role in the initiation of glycogen synthesis. Based on the structural modeling, the mutation can destabilize the structure and result in protein malfunctioning. Furthermore, in vitro experiments showed mutant GYG2 was unable to undergo the self-glucosylation, which is observed in wild-type GYG2. This is the first report of *GYG2* mutation in human, implying a possible link between GYG2 abnormality and LS.

Introduction

Glycogen is a large branched polysaccharide containing linear chains of glucose residues. Glycogen deposits in skeletal muscle and liver serve as shorter-term energy storage in mammals, while fat provides long-term storage. Glycogen biosynthesis begins with self-glucosylation of glycogenins by covalent binding of UDP-glucose to tyrosine residues of the glycogenins and the subsequent extension of approximately ten glucose residues (Pitcher et al. 1988; Smythe et al. 1988). Glycogen particles are formed by the continued addition of UDP-glucose to the growing

Electronic supplementary material The online version of this article (doi:10.1007/s00439-013-1372-6) contains supplementary material, which is available to authorized users.

E. Imagawa · M. Nakashima · Y. Tsurusaki · H. Saitsu · N. Matsumoto (✉) · N. Miyake (✉)
Department of Human Genetics, Yokohama City University Graduate School of Medicine, Yokohama 236-0004, Japan
e-mail: naomat@yokohama-cu.ac.jp

N. Miyake
e-mail: nmiyake@yokohama-cu.ac.jp

H. Osaka
Division of Neurology, Clinical Research Institute, Kanagawa Children's Medical Center, Yokohama 232-8555, Japan

A. Yamashita
Department of Molecular Biology, Yokohama City University School of Medicine, Yokohama 236-0004, Japan

M. Shiina · K. Ogata
Department of Biochemistry, Yokohama City University Graduate School of Medicine, Yokohama 236-0004, Japan

E. Takahashi
Division of Infection and Immunology, Clinical Research Institute, Kanagawa Children's Medical Center, Yokohama 232-8555, Japan

H. Sugie
Department of Pediatrics, Jichi Medical University, Tochigi 329-0498, Japan

glycogen chain by glycogen synthase, and introduction of branches every 10–14 residues by the glycogen branching enzyme (Krisman and Barengo 1975; Larner 1953). To date, two glycogenin paralogues have been identified in human, glycogenin-1 (GYG1) and glycogenin-2 (GYG2). These proteins have been shown to form homodimers, heterodimers and larger oligomers (Gibbons et al. 2002). GYG1 (muscle form) is expressed predominantly in muscle while GYG2 (liver form) is expressed mainly in liver, heart and pancreas (Barbetti et al. 1996; Mu et al. 1997). Biallelic GYG1 abnormality is known to cause muscle weakness and cardiac arrhythmia in humans through GYG1 autoglucosylation failure (Moslemi et al. 2010). However, human disease due to GYG2 abnormality has never been reported.

Leigh syndrome (LS; MIM #256000) was first described as a subacute necrotizing encephalomyelopathy by Dr. Denis Leigh in 1951 (Leigh 1951). LS is a progressive neurodegenerative disorder with an estimated incidence of 1:40,000 live births (Rahman et al. 1996). Onset is usually in early childhood (typically before age 2) (Naess et al. 2009; Ostergaard et al. 2007). Clinical manifestations of LS are observed in the central nervous system (CNS) (developmental delay, hypotonia, ataxia, convulsion, nystagmus, respiratory failure and dysphagia), peripheral nervous system (polyneuropathy and myopathy) and extraneural organs (deafness, diabetes, cardiomyopathy, kidney malfunction and others) (Finsterer 2008). The neurological features depend on the affected regions and degree of severity. The presence of bilateral, symmetrical, focal hyperintense T2-weighted MRI signals in basal ganglia (mainly putamen), thalamus, substantia nigra, substantia ruber, brainstem, cerebellum, cerebral white matter or spinal cord is diagnostic of LS (Farina et al. 2002; Medina et al. 1990). Neuropathological studies revealed that these lesions reflect neuronal necrosis, gliosis and vascular proliferation (Brown and Squier 1996; Leigh 1951). In the majority of LS cases, lactate, pyruvate or the lactate/pyruvate ratio is increased in blood and cerebrospinal fluid (Finsterer 2008). To the best of our knowledge, 37 nuclear genes are known to be mutated in LS, in addition to some mitochondrial genes (Antonicka et al. 2010; Debray et al. 2011; Finsterer 2008; Lopez et al. 2006; Martin et al. 2005; Quinonez et al. 2013). Thus, inheritance patterns of LS include mitochondrial, autosomal recessive and X-linked recessive modes (Benke et al. 1982; van Erven et al. 1987).

We encountered a Japanese family with affected brothers showing atypical LS without marked elevation of lactic or pyruvic acid and unknown etiology. A unique genetic variant was identified by whole exome sequencing (WES), which may be associated with atypical LS phenotype in this family.

Materials and methods

Subjects

Peripheral blood samples of affected brothers diagnosed with LS and their parents were collected after obtaining written informed consent. DNA was extracted from peripheral blood leukocytes using QuickGene-610L (Fujifilm, Tokyo, Japan) according to the manufacturer's instructions. Lymphoblastoid cell lines derived from all family members were established. The Institutional Review Boards of Yokohama City University School of Medicine approved this study.

Causative gene identification

Whole exome sequencing was performed in two affected individuals (II-2 and II-3 in Fig. 1a) as described in the Supplementary methods. All candidate variants based on autosomal and X-linked recessive models were checked by Sanger sequencing in the parents and affected siblings. PCR products amplified with genomic DNA as a template were sequenced on an ABI3500xl autosequencer (Applied Biosystems, Foster City, CA) and analyzed using Sequencher 5.0 (Gene Codes Corporation, Ann Arbor, MI). As the pedigree tree might also indicate mitochondrial inheritance of this disease and LS is known to be caused by mitochondrial genome mutations, we screened the entire mitochondrial genome by the algorithm reported previously (Picardi and Pesole 2012), using exome data (detailed in Supplementary methods).

Structure modeling

To evaluate the effect of the GYG2 missense mutation (c.665G>C, p.W222S in isoform a: NM_001079855) on its function at the molecular structural level, the mutated molecular structure was constructed, and the free energy change caused by the mutation was calculated using the FoldX software (version 3.0) (Guerois et al. 2002; Khan and Vihinen 2010). As crystal structure of human GYG2 is unavailable, that of human GYG1 (Protein Data Bank code; 3T7O) was used as a structural model. The mutation was introduced into one subunit of the GYG1 homodimer. The ligands included in the crystal structure of GYG1 were ignored in the calculation, because the FoldX energy function could not deal with the ligands. The calculation was repeated three times, and the resultant data were presented as an average value with standard deviations.

Preparation for mammalian expression vectors

Human glycogenin-2 isoform a cDNA clone (IMAGE Clone ID: 100008747) integrated in pENTR221 was purchased from Kazusa DNA Research Institute (Chiba, Japan). The

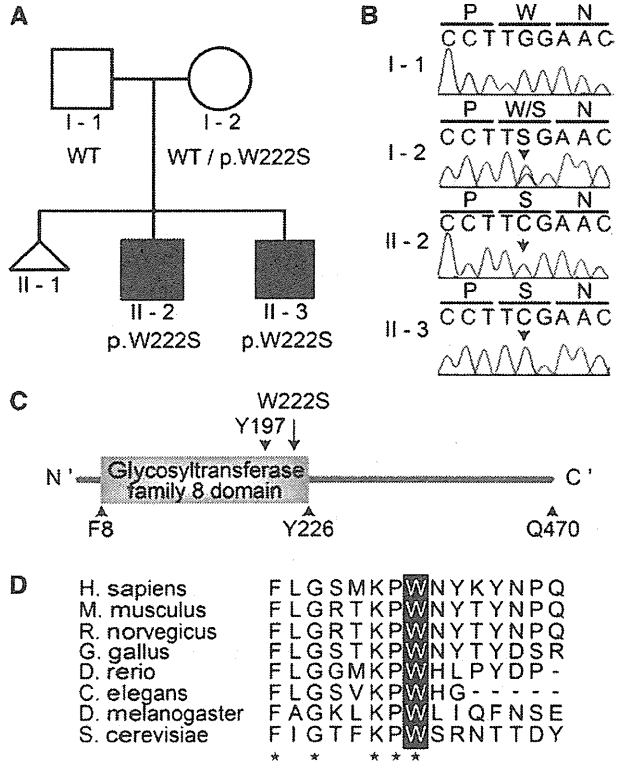

Fig. 1 Mutation Analysis of *GYG2*. **a** Pedigree of the family with a unique type of LS and a *GYG2* mutation (c.665G>C, p.W222S). *Square*, *circle* and *triangle* denote male, female and spontaneous abortion, respectively. *White* and *black symbols* indicate unaffected and affected individuals, respectively, while the affection status of the spontaneous abortion is unknown. **b** Electropherograms of a *GYG2* mutation. **c** The functional domain of human GYG2 (isoform a). The substitution of p.W222S is located within the glycosyltransferase family 8 domain (*yellow square*). **d** The evolutionary conservation of the W222 in GYG2. *Red stars* indicate identical amino acids from *S. cerevisiae* to *H. sapiens*. Sequences were aligned using CLUSTALW (http://www.genome.jp/tools/clustalw/)

missense mutation (c.665G>C, p.W222S) was introduced by Site-directed mutagenesis using the QuikChange II XL site-directed mutagenesis kit (Agilent Technologies, Santa Clara, CA). Wild-type and mutant C' V5/6xHis tagged GYG2 constructs were created using pcDNA-DEST40 (Invitrogen, Carlsbad, CA) by LR recombination in Gateway system (Invitrogen). To create the untagged construct, the last codon was altered to a stop codon by mutagenesis.

Self-glucosylation analysis

Glucosyltransferase activity of GYG2 was measured as previously described (Lomako et al. 1988), with slight modifications. In brief, COS-1 cells were maintained in Dulbecco's modified Eagle's medium (DMEM) (Sigma-Aldrich, Schnelldorf, Germany) containing 10 % heat-inactivated fetal bovine serum (FBS) (Gibco-BRL, Grand Island, NY), 2 mM L-glutamine (Sigma-Aldrich) and 1 % penicillin–streptomycin (Sigma-Aldrich). As previously described (Mu and Roach 1998), the ~80 % confluent COS-1 cells (~1 × 10^7) were transiently transfected by X-treamGENE9 DNA transfection reagent (Roche Applied Science, Foster City, CA) with 5 μg of either a wild-type Human GYG2 (isoform a) expressing plasmid or the same plasmid into which the W222S encoding mutation had been introduced. After 24 h, the cells were collected and lysed in 300 μl of buffer consisting of 50 mM HEPES, 0.5 % Triton X-100, 1 × EDTA-free protease Inhibitor Cocktail tablets (Roche Applied Science), 1 × phosphatase inhibitor cocktail (Nacalai Tesque Inc., Kyoto, Japan) and 0.5 mM β-mercaptoethanol (Mu et al. 1997). After centrifugation at 14,000 rpm for 15 min, 10 μl of the soluble fractions were mixed with 10 μl of 2 × reaction buffer containing 100 mM HEPES (pH7.5), 10 mM MgCl, 4 mM dithiothreitol (DTT) and 40 μM UDP-[^{14}C]-glucose (250 mCi/mmol; PerkinElmer, Waltham, MA) (Cao et al. 1993). After incubation at 30 °C for 30 min, the reaction was stopped by addition of 20 μl of 2 × Laemmli sample buffer (Sigma-Aldrich) (Viskupic et al. 1992). 15 μl of each sample was subjected to SDS-polyacrylamide gel electrophoresis. After treatment with Gel drying solution (Bio-Rad Laboratories, Hercules, CA) for 30 min, gels were dried. Dried gels were then exposed on X-ray film for 2 weeks to detect the incorporation of UDP-[^{14}C]-glucose into GYG2. In addition, the ^{14}C-signal intensities were evaluated using an imaging analyzer, BAS2500 (Fujifilm). Three independent experiments were performed.

Western blot analysis

For the detection of GYG2 protein, rabbit polyclonal anti-GYG2 antibodies (1:500 dilution; Abcam Inc., Cat.#HPA005495, Cambridge, MA) and horse-radish peroxidase (HRP)-conjugated anti-rabbit IgG (1:10,000 dilution; Jackson ImmunoResearch, Cat.#111-035-003, West Grove, PA) were used. Immunoblot chemiluminescence was performed using SuperSignal West Dura as substrate (Thermo Fisher Scientific, Waltham, MA). The chemiluminescence signal images were captured by FluorChem 8900 (Alpha Innotech, San Leandro, CA). Signal intensities were measured by AlphaEase FC (Alpha Innotech). Three independent experiments were performed.

Results

Clinical finding

Patient II-2 (Fig. 1a; Table 1) is a 26-year-old male born to non-consanguineous parents. His mother previously had a

Table 1 Clinical features of the presenting patients affected with LS

	II-2	II-3
Sex	M	M
Age (years)	26	19
Common clinical phenotype		
Psychomotor retardation	+	+
Failure to thrive	+	+
Swallowing difficulties	–	–
Spasticity	+	+
Rigidity	+	+
Pathological reflexes	+	+
Ataxia	+	+
Athetoid movements	+	+
Convulsions	+	+
Ophthalmoplegia	+	+
Strabismus	+	+
Gastrointestinal problems	+	+
Renal agenesis	NA	+
Pes equinovarus	+	+
Uncommon clinical phenotype		
Increase of ketone body	+	+

NA not assessed

spontaneous abortion. He was born at 39 weeks gestation without asphyxia after an uneventful pregnancy. His body weight was 3,680 g (+1.6 SD), his height was 50.0 cm (−0.5 SD), and his head circumference (HC) was 34.0 cm (−0.5 SD). His early developmental milestones were normal with head control and reach to toys at 4 months, roll at 6 months and grasp with two fingers at 7 months. At 10 months, he was referred to our hospital because of an inability to sit. His body weight was 9,120 g (±0.0 SD), his height was 76.0 cm (+1.3 SD), and his HC was 48.0 cm (+1.4 SD). He could smile and swallow well. Bilateral strabismus was noted. No minor anomalies were noticed. Muscle tone was normal. Deep tendon reflexes were normal with negative Babinski sign. He showed athetoid movements of trunk and extremities. He showed pes equinovarus at traction response. Levels of lactate and pyruvate were normal with 12.2 and 0.89 mg/dl (L/P ratio = 13.7), respectively. Other laboratory examinations, including blood gas, blood sugar, ammonia, AST, ALT, BUN, Creatine, TSH, T3, T4, amino acids, and urine organic acid analyses were all normal. Electroencephalogram (EEG) showed no abnormalities. He was suspected to have dyskinetic cerebral palsy and referred to the division of rehabilitation. He could crawl at the age of 2. At 6 years, he experienced a loss of consciousness followed by generalized tonic–clonic convulsion with fever and was admitted to another hospital. He was diagnosed with bilateral infarction of the basal ganglia. Although EEG showed no abnormalities, clonazepam was started with the suspicion of symptomatic epilepsy. At the age of 9, he was referred to us again. His weight was 19.1 kg (−4.5 SD), his height was 115.0 cm (−2.8 SD). He lost the ability to speak several words and switched handedness from right to left. He also showed other signs of regression: including spasticity with elevated deep tendon reflexes and positive Babinski sign. In addition, he suffered bilateral hip joint dislocations and the foot deformity became worse. Contractures were noted in all extremities. Brain magnetic resonance imaging (MRI) revealed a bilateral necrotic lesion of the globus pallidus (Fig. 2a, b). EEG and motor conduction velocities were normal. Laboratory examinations, including lactate and pyruvate, were all normal. At the age of 12, he was admitted with acute bronchitis, at that time he showed an increase of blood ketone bodies: acetoacetic acid, 720 μmol/l; 3OHBA, 974 μmol/l and urine ketone (+++). Blood levels of ammonia (18 μmol/l), sugar (125 mg/dl) and lactate/pyruvate (5.1/0.29 mg/dl) were all within normal range. The values of blood ketone bodies returned to normal level with the cease of fever. Deficiencies of 3-ketothiolase and succinyl-CoA:3-oxoacid CoA transferase were ruled out by enzyme analysis using fibroblasts. His clinical symptoms and repeated MRI show the non-progressive course of his disease. Currently he is unable to sit or speak any words. Despite the addition of carbamazepine and lamotrigine, he still exhibits generalized tonic–clonic convulsion a few times a year. He also takes medicine for hypertonicity including dantrolene sodium, diazepam, baclofen and levodopa.

Patient II-3 (Fig. 1a; Table 1), the younger brother of II-2, was born uneventfully. He was born at 37 week's gestation without asphyxia after an uneventful pregnancy. His body weight was 3,668 g (+1.5 SD), his height was 50.0 cm (+0.5 SD), and his HC was 36.0 cm (−0.5 SD). He suffered from bacterial meningitis of unknown origin at 1 month of age. He became unconscious followed by convulsion and gastroenteritis at 1 year and 11 months. Brain MRI showed marked swelling of the basal ganglia (Fig. 2c, d). He was diagnosed with bilateral infarction of the basal ganglia. After this event, he became left handed. When he was 2 years old, surgery was performed to correct bilateral inner strabismus. He was referred to our hospital at the age of 4 for evaluation. His body weight was 11.0 kg (−2.2 SD), his height was 92.5 cm (−1.2 SD), and his HC was 49.5 cm (−1.3 SD). He could respond with a smile to his mother's voice. Motor milestones were delayed with no head control. No minor anomalies were noticed. Muscle tone was hypotonic. Deep tendon reflexes were exaggerated with positive Babinski sign and ankle clonus. He showed pes equinovarus. He showed a significant increase of blood acetoacetic acid of 1,270 μmol/l and 3-OHBA of 3,270 μmol/l. Levels of blood lactate and pyruvate were normal (6.2 and 0.48 mg/dl, respectively, L/P ratio = 12.9).

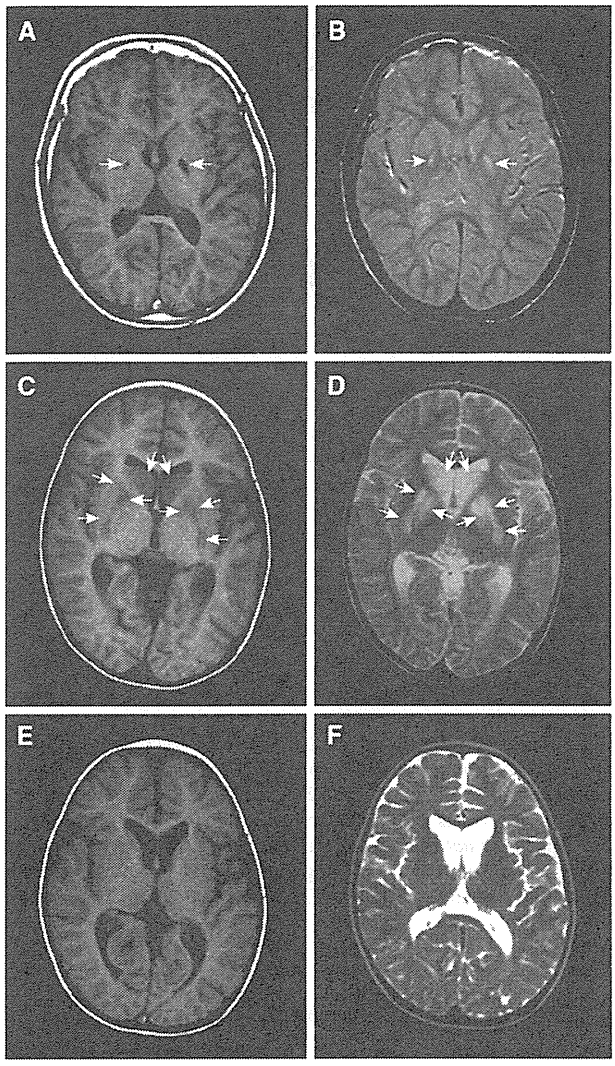

Fig. 2 Brain MRI of affected patients with a *GYG2* mutation. **a**, **b** (Patient II-2): T1 (**a**) and T2 (**b**) weighted brain magnetic resonance imaging (MRI) show necrotic lesion of bilateral globus pallidus (*arrows*). T2 elongation is observed at deep white matter at 1 year. **c**–**f** (Patient II-3): MRI at 1 year and 11 months shows swellings of caudate nuclei, globus pallidus, and putamen with the decreased T1 intensity (**c**) and increased T2 signals (**d**). *Arrows* indicate swollen lesions in basal ganglia. At 4 years (**e**, **f**), swelling of basal ganglia disappeared with continued mild high intensity in T2 weighted image (**f**)

Lactate and pyruvate levels of cerebrospinal fluid were slightly elevated with 11.3 and 1.11 mg/dl, respectively. Other laboratory examinations, including blood gas, blood sugar, ammonia, AST, ALT, BUN, Creatine, TSH, T3, T4, amino acids, and lysosomal enzymes were all normal. Urine organic acid analyses showed an increase of acetoacetic acid, 3-OHBA, and 3-OH-isovaleric acid. EEG showed no paroxysmal discharges. Muscle biopsy showed no specific abnormalities and no ragged red fibers. Staining for cytochrome c oxidase was normal (data not shown). Brain MRI disclosed T2 elongation in the basal ganglia and cerebral deep white matter (Fig. 2e, f). At the age of 5, he showed lethargy with fever. At 6 years, he again showed lethargy. Biochemical analysis disclosed a significant increase of blood ketone bodies: acetoacetic acid, 1,337 μmol/l; 3-OHBA, 4,845 μmol/l and urine ketone (+++). Blood levels of ammonia (28 μmol/l), sugar (78 mg/dl), lactate (5.1 mg/dl) and pyruvate (0.43 mg/dl) were all within normal range. Blood gas analysis revealed metabolic ketoacidosis with an increase of anion gap; 22.4 mEq/l (normal range 12 ± 2). His consciousness and biochemical measurements returned to normal within a few days with intravenous fluid infusion. Similar ketoacidosis attacks were repeatedly observed and agenesis of the left kidney and neurogenic bladder were recognized at the age of 8. He started intermittent urinary catheterization, and suffered from repeated urinary tract infections, resulted in chronic renal failure. Repeated brain MRI shows the progression of cerebral and cerebellar atrophy. He is now 19 years old and shows no gain of motor or intellectual abilities from the age of 4. He takes dantrolene sodium and diazepam for hypertonicity, and spherical charcoal, allopurinol for renal failure.

Identification of a *GYG2* variant by exome sequencing

A total of 2,433,011,483 bps (II-2) and 7,926,169,749 bps (II-3) were mapped to RefSeq coding DNA sequence (CDS). 83.3 and 96.0 % of CDS were covered by ten reads and more. We used only NGS data of II-3 for selecting candidate variants as the lower-quality NGS data of II-2 may lead to erroneous conclusion. Based on the hypothesis that this syndrome is inherited in an autosomal recessive or an X-linked recessive fashion, we focused on homozygous or compound heterozygous variants on autosomes and hemizygous variants on the X chromosome. While nine variants in four candidate genes were selected by in silico flow, only one hemizygous missense mutation in *GYG2* gene agreed with the familial segregation pattern (autosomal recessive or X-linked recessive) (Table S1, S2). The c.665G>C (p.W222S) in *GYG2* (isoform a: NM_001079855) was hemizygous in affected sibs and heterozygous in their mother, consistent with the X-linked recessive model, and was confirmed by Sanger sequence (Fig. 1b). The variant was absent in our in-house Japanese exome data ($n = 418$), the 1,000 Genomes database and ESP6500. Furthermore, no pathological variants in mtDNA were detected by exome sequence (Supplementary Results, Figure S1). In addition, a total of 21 LS patients (12 males and 9 females) were screened, but no pathological changes were found in *GYG2*.

GYG2 encodes GYG2 proteins with at least five isoforms: isoform a (NM_001079855), isoform b (NM_003918),

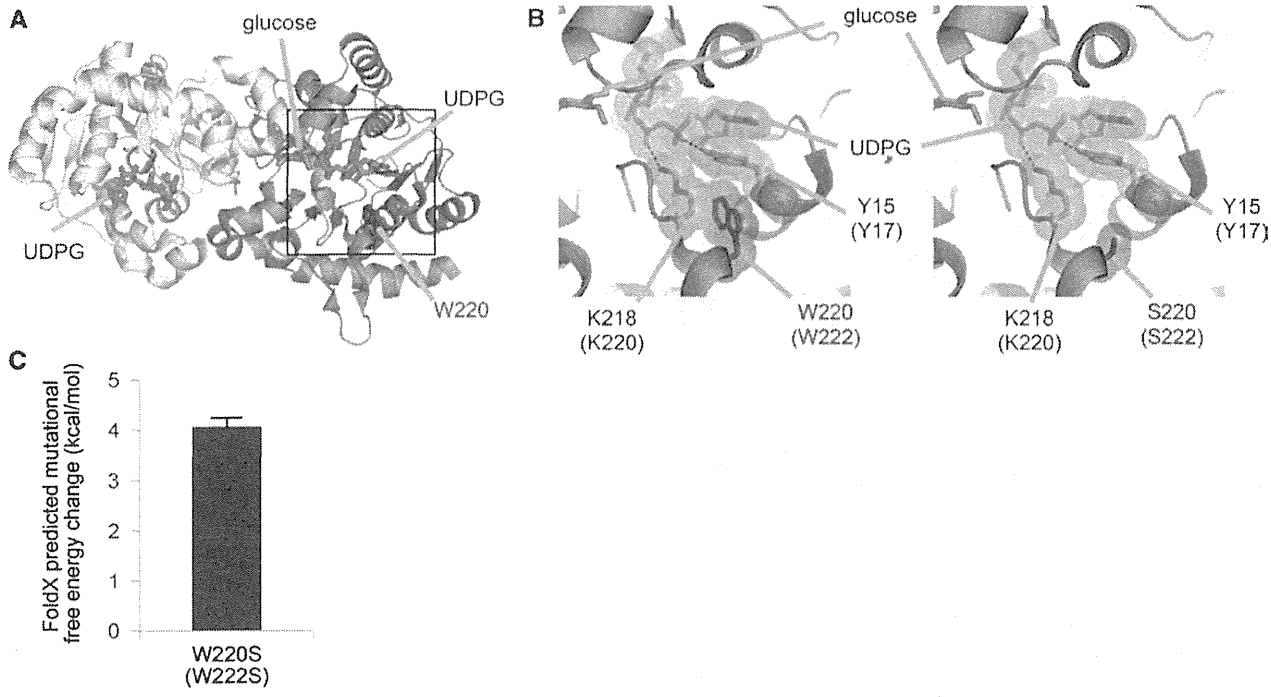

Fig. 3 Molecular structural consideration of the W222S mutation of GYG2. **a** Crystal structure of human GYG1 (Protein Data Bank code; 3T7O) (Chaikuad et al. 2011). Each monomer is colored *yellow* and *cyan*. α-helices, β-sheet and loops are drawn as *ribbons*, *arrows* and *threads*, respectively. The side chain of W222, glucose and UDP-glucose (UDPG) are shown as *sticks* in *red*, *orange* and *green*, respectively. Amino acid numbering shown is for human GYG1 with that for human GYG2 in *parenthesis*. The *squared area* corresponds to the close-up views in (**b**). **b** Detailed views of structures of the wild-type (*left*) and mutated GYG2 (p.W222S) (*right*). Amino acid residues at positions of 15, 218 and 220 and UDPG are shown as sticks with van der Waals representation and annotations. Hydrogen bonds are depicted as *dotted lines*. **c** Calculated free energy change upon the p.W222S mutation of GYG2 using FoldX software. All the molecular structures were drawn using PyMOL (www.pymol.org)

isoform c (NM_001184702), isoform d (NM_001184703), and isoform e (NM_001184704). At least two GYG2 isoforms (isoform a and b) are expressed preferentially in liver, heart and pancreas (Mu et al. 1997), while the detailed expression and function of other isoforms are undetermined. GYG2 has a glycosyltransferase family 8 domain and initiates glucose addition on its Tyrosine residue (Y197 in isoform a) via *O*-glycosylation (self-glucosylation) and can also attach an additional 7–10 residues of UDP-glucose to itself (Bollen et al. 1998; Lomako et al. 2004; Zhai et al. 2001). The W222 within the glycosyltransferase family 8 domain is evolutionarily highly conserved from *S. cerevisiae* to *H. sapiens* (Fig. 1c, d). In addition, all isoforms contain this residue. Thus, it is thought that this mutation may impair its biological function.

Structural consideration of the p.W222S mutation in human GYG2

The amino acid residue W222 of GYG2 (isoform a) was mapped to the crystal structure of human GYG1 (Chaikuad et al. 2011), since no experimental structure of GYG2 was available. W222 is involved in a hydrophobic core near the UDP-glucose (UDPG) binding site along with Y17 and K220 (Fig. 3a, b). The side chains of Y17 and K220 are hydrogen-bonded to UDPG, and the former also makes van der Waals contacts with the uridine ring of UDPG in a stacking mode. Therefore, the formation of the hydrophobic core appears to be a prerequisite for UDPG binding. To estimate the impact of the W222S mutation on the protein stability, we modeled the mutant structure and calculated the free energy change upon the mutation using the FoldX software. As a result, the mutation was predicted to destabilize the protein structure with about 4 kcal/mol increase in free energy (Fig. 3c). This suggests that the W222S mutation would impair UDPG binding (Fig. 3b).

Self-glucosylation analysis

To see the functional effects of the *GYG2* mutation in vitro, glucosyltransferase activity monitoring by self-glucosylation was measured using wild-type (WT) and W222S mutant (Mut) GYG2 (isoform a) transiently

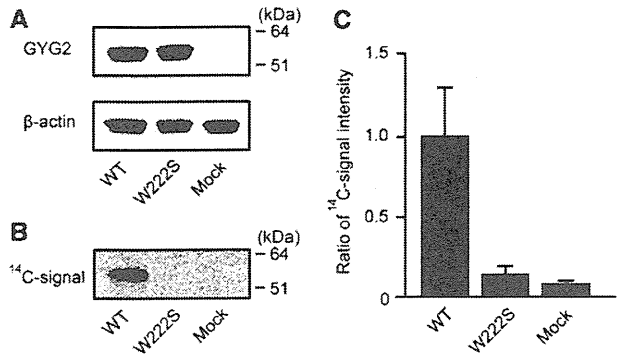

Fig. 4 Enzyme activity of GYG2. **a** Western blot analysis of recombinant GYG2. Wild-type (WT) and mutant (p.W222S) GYG2 was detected at the expected size (52 kDa). β-actin (42 kDa) was used as an internal control. **b** Autoradiography images presenting ^{14}C glucosylation toward GYG2. The signal was detected in WT, but undetected in mutant, with similar levels to Mock. **c** Graphic presentation of autoglucosylation of GYG2. The activity detected in Mock might be due to the endogenous glycogenin. *Error bars* represent the standard error of the mean

overexpressed in COS-1 cells. By immunoblotting, the expected 52 kDa bands of recombinant WT and Mut GYG2 were detected with similar expression levels (Fig. 4a). While WT GYG2 showed reasonable glucosyltransferase activity, Mut GYG2 almost completely lost the enzyme activity and was similar to the Mock level (Fig. 4b, c).

Expression analysis of GYG1 and GYG2

To observe tissue distribution of the human *GYG1* and *GYG2*, expression analysis was performed using multiple tissue cDNA panels. *GYG1* was expressed preferentially in skeletal muscle and heart from fetus to adult stages as previous reports (Barbetti et al. 1996). *GYG2* is dominantly expressed in liver from fetus through adult stages and moderately expressed in brain, heart, pancreas and kidney (Supplementary Results, Figure S2). To be marked, *GYG1* is not expressed in liver and brain where *GYG2* is highly expressed.

Discussion

In this study, we analyzed unique brothers affected with LS who were born to non-consanguineous healthy parents after uneventful pregnancies. Patient II-2 and II-3 developed LS accompanied by delayed developmental milestones at 10 months and 13 months of age, respectively. Their age of onset, clinical features and brain imaging were compatible with the diagnosis of LS. Interestingly, CNS abnormalities were observed (developmental delay, convulsion, athetoid movements, nystagmus, hypotonia, spasticity, increased deep tendon reflex and abnormal reflection), but involvement of peripheral nerve and extraneural organs was obscure. Based on the facts including (1) male (X-linked recessive), (2) normal lactate/pyruvate, (3) ketonemia/ketonuria, and (4) CNS predominant symptoms, the hemizygous *GYG2* mutation was highlighted a primary culprit.

In this study, we first identified a human *GYG2* mutation in affected brothers with LS with ketonemia/ketonuria but normal blood lactate/pyruvate. We can hypothesize a pathomechanism of the *GYG2* impairment in this family based on the canonical pathway of glycogen metabolism (Fig. 5). As glycogen storage in liver might be decreased because of the GYG2 malfunction, glucose is easily depleted. To keep appropriate blood glucose concentrations, the metabolism would be shifted toward gluconeogenesis and beta-oxidation to create glucose and energy sources like Acetyl-CoA (Garber et al. 1974; Laffel 1999; Randle et al. 1964). Excess beta-oxidation would result in overproduction of ketone bodies, consistent with the observation of ketonemia and ketonuria. However, pyruvate and lactate could be normally metabolized in gluconeogenesis and/or TCA cycle and would not accumulate in the body as seen in the majority of LS patients. Interestingly, both patients showed normal blood glucose level while showing LS manifestations which might be due to tissue energy depletion. In GYG2-deficient patients, the CNS was dominantly affected, while the effect of this abnormal metabolism was thought to extend to the entire body. This predominance could be explained by high glucose consumption as the primary energy source in brain (Amaral 2012; Magistretti and Pellerin 1999) and glycogen depletion in brain tissue level, while the blood sugar level was maintained by the other compensatory mechanism. This is similar to the muscle specific phenotypes (muscle weakness and arrhythmia) observed in patients with deficiencies of "muscle form" GYG1 in the absence of hypoglycemia (Moslemi et al. 2010). Remarkably, glycogen was less in the muscle tissue of GYG1 depleted patient (Moslemi et al. 2010). These evidences might indicate that it is not always linked between glucose level in the peripheral blood and glycogen/energy supply in tissue level while we could not show the loss of glycogen in liver or brain tissues because the materials were not available. In addition, deficiencies in two paralogous enzymes, GYG1 and GYG2, result in different human diseases suggesting they are unable to compensate each other in specific organs.

The *GYG2* mutation is probably causative for LS in this family. However, it is possible that the mutation is just coincidence because we just showed genetic evidences (due

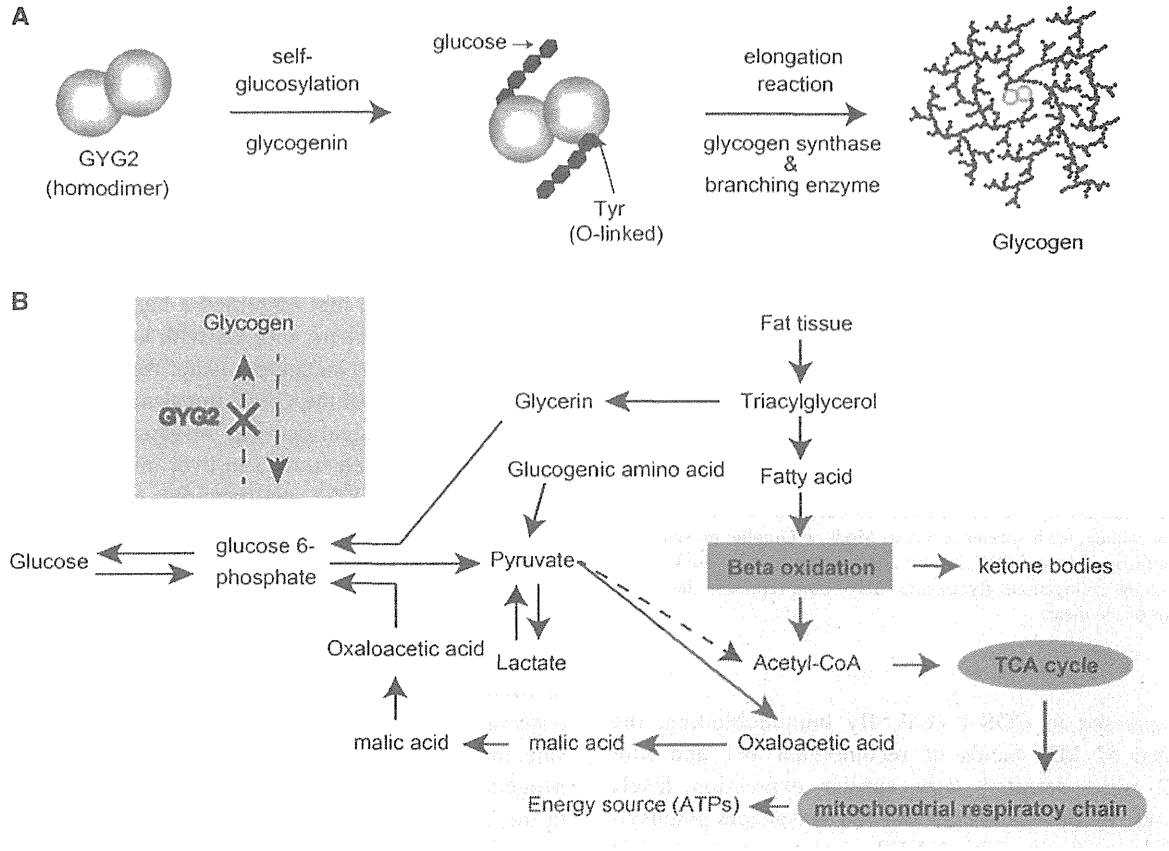

Fig. 5 Biochemical metabolisms in glycogen storage and glycolysis pathways. **a** Schematic presentation of glycogen biosynthesis. GYG2 has a catalytic capability for *O*-linked self-glucosylation at Tyrosine (Y197 in isoform a) and adds approximately 10 glucose molecules. By the subsequent elongating reactions by glycogen synthase and branching enzyme, giant molecule "glycogen" is formed. **b** Modeled biochemical pathway in GYG2 impairment. As the GYG2 impairment results in the absence of glycogen storage, glycogen is easy to be depleted and gluconeogenesis is induced from fat tissues and glucogenic amino acids. The reactions in mitochondria are shown in *yellow shadow*. While increased acetyl-CoA inhibits the pyruvate dehydrogenase complex which irreversibly converts pyruvate to acetyl-CoA (as shown as *dotted line*), it accelerates gluconeogenesis through pyruvate–oxaloacetic acid–malic acid–oxaloacetic acid. Triacylglycerol was metabolized into glycerin and fatty acid. Fatty acid was used for beta-oxidation and ketone production. The *arrows* indicate the directions of normal metabolism. *Red arrows* indicate the predicted predominant pathways in GYG2-deficient patients

to its rarity and familial co-segregation) and GYG2 loss of function by in vitro study without showing any sufficient data on how the *GYG2* mutation causes LS.

In conclusion, we describe the first human variant of *GYG2* which may be associated with the atypical LS phenotype in this family. Further studies are absolutely needed to conclude whether *GYG2* abnormality leads to atypical LS observed in this family.

Acknowledgments We thank all the patients and their families for participating in this work. We deeply appreciate Dr. Toshiyuki Fukao, who is the professor of Department of Pediatrics, Graduate School of Medicine, Gifu University, for the enzyme assay for 3-ketothiolase deficiency and succinyl-CoA:3-oxoacid CoA transferase. We would like to thank Dr. Yasushi Okazaki at Research Center for Genomic Medicine, Saitama Medical University for helpful discussion. We also thank Ms. Y. Yamashita, S. Sugimoto and K. Takabe for their technical assistance. This work was supported by research grants from the Ministry of Health, Labour, and Welfare (H. Saitsu, N. Matsumoto and N. Miyake), the Japan Science and Technology Agency (N. Matsumoto), the Strategic Research Program for Brain Sciences (to N. Matsumoto), a Grant-in-Aid for Scientific Research on Innovative Areas (Transcription Cycle) from the Ministry of Education, Culture, Sports, Science, and Technology of Japan (N. Matsumoto), a Grant-in-Aid for Scientific Research from the Japan Society for the Promotion of Science (to N. Matsumoto), a Grant-in-Aid for Young Scientists from the Japan Society for the Promotion of Science (H. Saitsu and N. Miyake), a grant from the 2012 Strategic Research Promotion of Yokohama City University (N. Matsumoto), and research grants from the Japan Epilepsy Research Foundation (H. Saitsu) and the Takeda Science Foundation (N. Matsumoto and N. Miyake).

Conflict of interest The authors declare that they have no conflict of interest.

References

Amaral AI (2012) Effects of hypoglycaemia on neuronal metabolism in the adult brain: role of alternative substrates to glucose. J Inherit Metab Dis. doi:10.1007/s10545-012-9553-3

Antonicka H, Ostergaard E, Sasarman F, Weraarpachai W, Wibrand F, Pedersen AM, Rodenburg RJ, van der Knaap MS, Smeitink JA, Chrzanowska-Lightowlers ZM, Shoubridge EA (2010) Mutations in C12orf65 in patients with encephalomyopathy and a mitochondrial translation defect. Am J Hum Genet 87:115–122. doi:10.1016/j.ajhg.2010.06.004

Barbetti F, Rocchi M, Bossolasco M, Cordera R, Sbraccia P, Finelli P, Consalez GG (1996) The human skeletal muscle glycogenin gene: cDNA, tissue expression and chromosomal localization. Biochem Biophys Res Commun 220:72–77. doi:10.1006/bbrc.1996.0359

Benke PJ, Parker JC Jr, Lubs ML, Benkendorf J, Feuer AE (1982) X-linked Leigh's syndrome. Hum Genet 62:52–59

Bollen M, Keppens S, Stalmans W (1998) Specific features of glycogen metabolism in the liver. Biochem J 336:19–31

Brown GK, Squier MV (1996) Neuropathology and pathogenesis of mitochondrial diseases. J Inherit Metab Dis 19:553–572

Cao Y, Mahrenholz AM, DePaoli-Roach AA, Roach PJ (1993) Characterization of rabbit skeletal muscle glycogenin. Tyrosine 194 is essential for function. J Biol Chem 268:14687–14693

Chaikuad A, Froese DS, Berridge G, von Delft F, Oppermann U, Yue WW (2011) Conformational plasticity of glycogenin and its maltosaccharide substrate during glycogen biogenesis. Proc Natl Acad Sci USA 108:21028–21033. doi:10.1073/pnas.1113921108

Debray FG, Morin C, Janvier A, Villeneuve J, Maranda B, Laframboise R, Lacroix J, Decarie JC, Robitaille Y, Lambert M, Robinson BH, Mitchell GA (2011) LRPPRC mutations cause a phenotypically distinct form of Leigh syndrome with cytochrome c oxidase deficiency. J Med Genet 48:183–189. doi:10.1136/jmg.2010.081976

Farina L, Chiapparini L, Uziel G, Bugiani M, Zeviani M, Savoiardo M (2002) MR findings in Leigh syndrome with COX deficiency and SURF-1 mutations. AJNR Am J Neuroradiol 23:1095–1100

Finsterer J (2008) Leigh and Leigh-like syndrome in children and adults. Pediatr Neurol 39:223–235. doi:10.1016/j.pediatrneurol.2008.07.013

Garber AJ, Menzel PH, Boden G, Owen OE (1974) Hepatic ketogenesis and gluconeogenesis in humans. J Clin Invest 54:981–989. doi:10.1172/JCI107839

Gibbons BJ, Roach PJ, Hurley TD (2002) Crystal structure of the autocatalytic initiator of glycogen biosynthesis, glycogenin. J Mol Biol 319:463–477. doi:10.1016/S0022-2836(02)00305-4

Guerois R, Nielsen JE, Serrano L (2002) Predicting changes in the stability of proteins and protein complexes: a study of more than 1000 mutations. J Mol Biol 320:369–387. doi:10.1016/S0022-2836(02)00442-4

Khan S, Vihinen M (2010) Performance of protein stability predictors. Hum Mutat 31:675–684. doi:10.1002/humu.21242

Krisman CR, Barengo R (1975) A precursor of glycogen biosynthesis: alpha-1,4-glucan-protein. Eur J Biochem 52:117–123

Laffel L (1999) Ketone bodies: a review of physiology, pathophysiology and application of monitoring to diabetes. Diabetes Metab Res Rev 15:412–426

Larner J (1953) The action of branching enzymes on outer chains of glycogen. J Biol Chem 202:491–503

Leigh D (1951) Subacute necrotizing encephalomyelopathy in an infant. J Neurol Neurosurg Psychiatry 14:216–221

Lomako J, Lomako WM, Whelan WJ (1988) A self-glucosylating protein is the primer for rabbit muscle glycogen biosynthesis. FASEB J 2:3097–3103

Lomako J, Lomako WM, Whelan WJ (2004) Glycogenin: the primer for mammalian and yeast glycogen synthesis. Biochim Biophys Acta 1673:45–55. doi:10.1016/j.bbagen.2004.03.017

Lopez LC, Schuelke M, Quinzii CM, Kanki T, Rodenburg RJ, Naini A, Dimauro S, Hirano M (2006) Leigh syndrome with nephropathy and CoQ10 deficiency due to decaprenyl diphosphate synthase subunit 2 (PDSS2) mutations. Am J Hum Genet 79:1125–1129. doi:10.1086/510023

Magistretti PJ, Pellerin L (1999) Cellular mechanisms of brain energy metabolism and their relevance to functional brain imaging. Philos Trans R Soc Lond B Biol Sci 354:1155–1163. doi:10.1098/rstb.1999.0471

Martin MA, Blazquez A, Gutierrez-Solana LG, Fernandez-Moreira D, Briones P, Andreu AL, Garesse R, Campos Y, Arenas J (2005) Leigh syndrome associated with mitochondrial complex I deficiency due to a novel mutation in the NDUFS1 gene. Arch Neurol 62:659–661. doi:10.1001/archneur.62.4.659

Medina L, Chi TL, DeVivo DC, Hilal SK (1990) MR findings in patients with subacute necrotizing encephalomyelopathy (Leigh syndrome): correlation with biochemical defect. AJR Am J Roentgenol 154:1269–1274

Moslemi AR, Lindberg C, Nilsson J, Tajsharghi H, Andersson B, Oldfors A (2010) Glycogenin-1 deficiency and inactivated priming of glycogen synthesis. N Engl J Med 362:1203–1210. doi:10.1056/NEJMoa0900661

Mu J, Roach PJ (1998) Characterization of human glycogenin-2, a self-glucosylating initiator of liver glycogen metabolism. J Biol Chem 273:34850–34856

Mu J, Skurat AV, Roach PJ (1997) Glycogenin-2, a novel self-glucosylating protein involved in liver glycogen biosynthesis. J Biol Chem 272:27589–27597

Naess K, Freyer C, Bruhn H, Wibom R, Malm G, Nennesmo I, von Dobeln U, Larsson NG (2009) MtDNA mutations are a common cause of severe disease phenotypes in children with Leigh syndrome. Biochim Biophys Acta 1787:484–490. doi:10.1016/j.bbabio.2008.11.014

Ostergaard E, Hansen FJ, Sorensen N, Duno M, Vissing J, Larsen PL, Faeroe O, Thorgrimsson S, Wibrand F, Christensen E, Schwartz M (2007) Mitochondrial encephalomyopathy with elevated methylmalonic acid is caused by SUCLA2 mutations. Brain 130:853–861. doi:10.1093/brain/awl383

Picardi E, Pesole G (2012) Mitochondrial genomes gleaned from human whole-exome sequencing. Nat Methods 9:523–524. doi:10.1038/nmeth.2029

Pitcher J, Smythe C, Cohen P (1988) Glycogenin is the priming glucosyltransferase required for the initiation of glycogen biogenesis in rabbit skeletal muscle. Eur J Biochem 176:391–395

Quinonez SC, Leber SM, Martin DM, Thoene JG, Bedoyan JK (2013) Leigh syndrome in a girl with a novel DLD mutation causing E3 deficiency. Pediatr Neurol 48:67–72. doi:10.1016/j.pediatrneurol.2012.09.013

Rahman S, Blok RB, Dahl HH, Danks DM, Kirby DM, Chow CW, Christodoulou J, Thorburn DR (1996) Leigh syndrome: clinical features and biochemical and DNA abnormalities. Ann Neurol 39:343–351. doi:10.1002/ana.410390311

Randle PJ, Newsholme EA, Garland PB (1964) Regulation of glucose uptake by muscle. 8. Effects of fatty acids, ketone bodies and pyruvate, and of alloxan-diabetes and starvation, on the uptake and metabolic fate of glucose in rat heart and diaphragm muscles. Biochem J 93:652–665

Smythe C, Caudwell FB, Ferguson M, Cohen P (1988) Isolation and structural analysis of a peptide containing the novel tyrosyl-glucose linkage in glycogenin. EMBO J 7:2681–2686

van Erven PM, Cillessen JP, Eekhoff EM, Gabreels FJ, Doesburg WH, Lemmens WA, Slooff JL, Renier WO, Ruitenbeek W (1987)

Leigh syndrome, a mitochondrial encephalo(myo)pathy. A review of the literature. Clin Neurol Neurosurg 89:217–230

Viskupic E, Cao Y, Zhang W, Cheng C, DePaoli-Roach AA, Roach PJ (1992) Rabbit skeletal muscle glycogenin. Molecular cloning and production of fully functional protein in Escherichia coli. J Biol Chem 267:25759–25763

Zhai L, Schroeder J, Skurat AV, Roach PJ (2001) Do rodents have a gene encoding glycogenin-2, the liver isoform of the self-glucosylating initiator of glycogen synthesis? IUBMB Life 51:87–91. doi:10.1080/15216540117315

[10] Hueber W, Sands BE, Lewitzky S, Vandemeulebroecke M, Reinisch W, Higgins PD, et al. Secukinumab, a human anti-IL-17A monoclonal antibody, for moderate to severe Crohn's disease: unexpected results of a randomised, double-blind placebo-controlled trial. Gut 2012;61:1693–700.

Jiang Zhou, Frieder Koszik
Patrick Brunner
Georg Stingl*
Division of Immunology, Allergy and Infectious Diseases (DIAID), Department of Dermatology, Medical University of Vienna, Vienna, Austria

* Corresponding author at: Department of Dermatology, Division of Immunology, Allergy and Infectious Diseases (DIAID), Medical University of Vienna, Waehringer Guertel 18-20, 1090 Vienna, Austria. Tel.: 43 1 403 6933; fax: 43 1 405 1288.
E-mail address: georg.stingl@meduniwien.ac.at (G. Stingl).

Received 9 December 2013
Received in revised form 12 May 2014
Accepted 13 May 2014

http://dx.doi.org/10.1016/j.jdermsci.2014.05.006

Letter to the Editor

The complete type of pachydermoperiostosis: A novel nonsense mutation p.E141* of the *SLCO2A1* gene

Pachydermoperiostosis (PDP), or primary hypertrophic osteoarthropathy (PHO: MIM: 167100), is a rare genetic disease affecting both skin and bones. The major diagnostic criteria include finger clubbing, periostosis, pachydermia, and cutis verticis gyrata (CVG). Additional symptoms, including sebaceous hyperplasia, hyperhidrosis, and arthropathy have been reported [1,2].

A homozygous mutation in *HPGD*, which encodes 15-hydroxyprostaglandin dehydrogenase (15-PGDH), leads to PHO and PDP [3]. However, PHO and PDP are genetically heterogeneous. Whole exome analysis of PDP in Japanese, Chinese, Caucasian, and other populations has revealed homozygous mutations in the solute carrier organic anion transporter family member 2A1 (*SLCO2A1*) gene, encoding prostaglandin transporter (PGT) [4–6]. Increased tissue levels of prostaglandin E2 (PGE2) resulting from defective degradation contribute to the pathogenesis of PHO and PDP. A genetic defect in either *SLCO2A1* or *HPGD* can cause PHO and PDP. These observations enabled us to categorize the disease into two types: (1) PHOAR1, MIM: 259100, caused by *HPGD* deficiency, and (2) PHOAR2, MIM: 614441, caused by *SLCO2A1* deficiency. Whereas the male to female ratio is approximately 1 for PHOAR1, no female patients have presented with the typical skin and bone manifestations of PHOAR2 [7]. We previously reported a female *SLCO2A1*-deficient PDP patient with minimal pachydermia [8].

We herein report four cases of complete type of pachydermoperiostosis carrying five different *SLCO2A1* mutations including a novel mutation.

PDP was diagnosed according to established clinical and radiological criteria [1]. Individuals participating in the study provided written informed consent. This study was approved by the ethics committee of the National Center for Child Health and Development and Keio University School of Medicine. Serum and urinary levels of PGE2 were measured as described elsewhere [4]. Isolation of genomic DNA, amplification, sequencing, and screening for mutations of the *SLCO2A1* and *HPGD* genes have been described elsewhere [4].

We screened four PDP patients for *SLCO2A1* and *HPGD* mutations. Clinical features, gene mutations, and serum and urine levels of PGE2 are summarized in Table 1. The study population comprised of only men (age range, 19–25 years). No participant had a family history of PDP, and all had non-consanguineous parents. Their medical histories have been provided in the Supplementary data.

All four patients were compound heterozygous for *SLCO2A1* mutations (Table 1). We identified five different mutations, of which c.421G>T/p.E141* was novel (Fig. 1, and Supplementary Fig. 3). No *HPGD* mutation was found.

Table 1
Summary of clinical phenotype, *SLCO2A1* mutations, and PGE2.

Case	P1	P2	P3	P4
Current age (years)	19	21	20	20
Onset age (years)	15	16	14	14
Gender	M	M	M	M
Clinical subtype	Complete	Complete	Complete	Complete
HPGD	ND	ND	ND	ND
SLCO2A1 allele 1	c.940+1G>A p.R288Gfs*7	c.1807C>T p.R603*	c.940+1G>A p.R288Gfs*7	c.940+1G>A p.R288Gfs*7
SLCO2A1 allele 2	c.1279_1290del12 p.E427_P430del	c.754C>T p.R252*	c.421G>T p.E141*	c.1807C>T p.R603*
Serum PGE2 (pg/ml)[a]	337	127	256	NA
Urinary PGE2 (pg/ml)	264	895	3688	NA
Triad				
Digital clubbing	+	+	+	+
Periostosis	+	+	+	+
Pachydermia	+	+	+	+
Cutis verticis gyrata	+	+	+	+
Skin				
Palmar and plantar hyperhidrosis	+	+	+	–
Acne	+	+	+	+
Seborrhoea and eczema	+	–	+	+
Skeletal				
History of bone fractures	–	–	+	–
Swelling of large joints	+	+	+	+
Painful joints on exercise	–	+	–	+
Hydrarthrosis	+	+	+	+

All patients except for P4 had no history of peptic ulcers and anemia. M: male, ND: (tested but) not detected, NA: not available, +: positive, –: negative or unknown.
[a] normal range: 25–200 pg/ml.

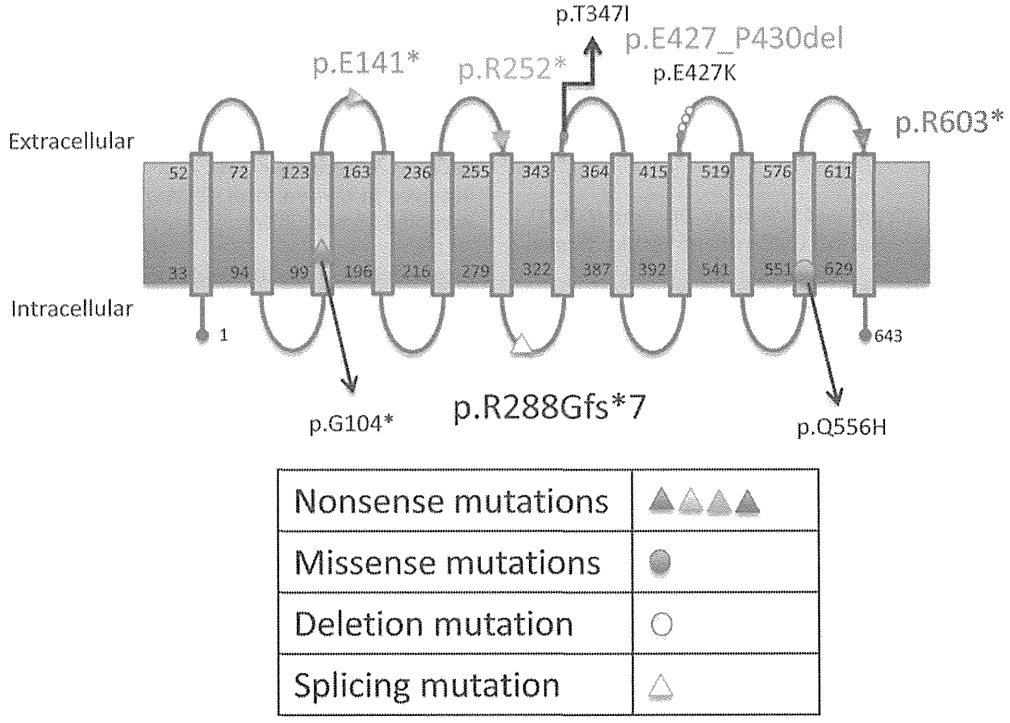

Fig. 1. Schematic representation of the prostaglandin transporter protein. The positions of the mutations of the *SLCO2A1* gene in Japanese patients with pachydermoperiostosis are depicted [4,8]. The green arrowhead indicates the position of the novel nonsense mutation p.E141* in this study.

SLCO2A1 mutation screening of Patient (P) 1 revealed compound heterozygous mutations c.940 + 1 G > A and c.1279_1290del12; the heterozygous mutation c.940 + 1 G > A was located in the splice donor site of intron 7, which resulted in the loss of exon 7 and a truncation of PGT [4]. The heterozygous c.1279_1290del12 mutation in exon 9 resulted in the deletion of four amino acids at positions 427–430 (p.427_430del). The proband's mother was heterozygous for c.1279_1290del12 (Supplementary Fig. 1F).

P2 was compound heterozygous for c.1807C > T in exon 13, and c.754C > T in exon 6 introduced a stop codon at position 603 (p.R603*) and 252 (p.R252*), respectively [8,9]. The proband's family was not available (Supplementary Fig. 2E).

P3 was compound heterozygous for c.940 + 1 G > A and c.421G > T; the heterozygous mutation c.421G > T in exon 4 introduced a stop codon at position 141 (p.E141*). This mutation probably decreases PGT function. The proband's mother was heterozygous for c.940 + 1 G > A (Supplementary Fig. 3E).

P4 was compound heterozygous for c.940 + 1 G > A and c.754C > T as found in P1 and P2. The proband's family was not available (Supplementary Fig. 4E).

It is unlikely that the serum level of PGE2 is useful for differential diagnosis of the disease, as the serum level of P2 was within normal limits. By contrast, the urinary level of PGE2 appeared to be associated with the disease, but we did not correct the measurement value by the urinary concentration of creatinine, which was not available in this study (Table 1).

We diagnosed P1 as complete PDP because of the CVG. The *SLCO2A1* mutations (c.940 + 1 G > A and c.1279_1290del12) were identical to those of P1 in our previous report (Sasaki's P1) [4]. Magnetic resonance imaging (MRI) showed vertex scalp folds in Sasaki's P1, indicating CVG (unpublished observation). We thus diagnosed a conversion from the incomplete type to the complete type. This relatively mild phenotype of CVG observed in these two patients can be explained by assuming that the four-amino-acid deletion mutant protein p.E427_P430del has partial PGT activity as discussed in our previous report [4]. Seifert et al. [9] observed that patients with homozygous *SLCO2A1* mutations developed manifestations of PHO later than patients with *HPGD* mutations. Similar to PDP, symptoms began with clubbing of the distal phalanges during puberty, followed by pachydermia shortly after puberty. However, patients with homozygous *SLCO2A1* mutations showed more arthritis, joint involvement, and pachydermia than those with homozygous or compound heterozygous *HPGD* mutations. In this regard, clinical diagnosis of the type of PDP should be tentative in early childhood. Based on the *SLCO2A1* gene mutations in Japanese patients found in this study, the diagnosis may change after puberty, as seen in P1.

Except for P1, who had an atypical phenotype, three of four patients in the present study carried the *SLCO2A1* mutation, which resulted in a premature stop codon (p.R603*; p.R252*; p.E141*). Quantitative PCR revealed a significant reduction of the *SLCO2A1* mRNA level in cultured fibroblasts obtained from the patient carrying the mutation p.R252*, suggesting nonsense-mediated decay [9]. It has not been reported whether the novel mutation p.E141* and the recently discovered mutation p.R603* affect the *SLCO2A1* mRNA level. Further analyses are necessary whether these mutations introduce a truncation or deficiency of PGT leading to more severe phenotypes of PDP.

In conclusion, we found five different *SLCO2A1* mutations including a new mutation p.E141* in the complete type of pachydermoperiostosis.

Conflicts of interest

None declared.

Acknowledgements

We thank the patients and their families for their generous cooperation. We also thank Ms. A. Maruta for secretarial assistance and Ms. M. Furuhashi for her excellent technical assistance.

This work was supported by grants from the Ministry of Health, Labour and Welfare of Japan to H. Niizeki (Research for Intractable Diseases) and a grant from Keio University to J. Kudoh.